Scientific Reports

https://doi.org/10.1038/s41598-026-62577-1

Article in Press

Improved adaptation mechanism in MRAC scheme with nonlinear reference model for nonlinear uncertain systems

Received: 25 April 2026

Accepted: 13 July 2026

Published online: 07 August 2026

Cite this article as: Kocagil B.M., Çopur E.H. & Salamci M.U. Improved adaptation mechanism in MRAC scheme with nonlinear reference model for nonlinear uncertain systems. *Sci Rep* (2026). https://doi.org/10.1038/s41598-026-62577-1

Bedrettin Mahmut Kocagil, Engin Hasan Çopur & Metin U. Salamci

We are providing an unedited version of this manuscript to give early access to its findings. Before final publication, the manuscript will undergo further editing. Please note there may be errors present which affect the content, and all legal disclaimers apply.

If this paper is publishing under a Transparent Peer Review model then Peer Review reports will publish with the final article.

ARTICLE IN PRESS

© The Author(s) 2026. **Open Access** This article is licensed under a Creative Commons Attribution 4.0 International License, which permits use, sharing, adaptation, distribution and reproduction in any medium or format, as long as you give appropriate credit to the original author(s) and the source, provide a link to the Creative Commons licence, and indicate if changes were made. The images or other third party material in this article are included in the article's Creative Commons licence, unless indicated otherwise in a credit line to the material. If material is not included in the article's Creative Commons licence and your intended use is not permitted by statutory regulation or exceeds the permitted use, you will need to obtain permission directly from the copyright holder. To view a copy of this licence, visit http://creativecommons.org/licenses/by/4.0/.

ARTICLE IN PRESS

Improved Adaptation Mechanism in MRAC Scheme with Nonlinear Reference Model for Nonlinear Uncertain Systems

Bedrettin Mahmut Kocagil 0000-0003-4751-2508[1*],
Engin Hasan C¸opur 0000-0003-0837-1255[2] and Metin U. Salamci 0000-0002-6150-8014[3]

[1*]Department of Mechanical Engineering, Erzurum Technical University, Erzurum, 25100, Tu¨rkiye.
[2]Department of Aerospace Engineering, Necmettin Erbakan University, Konya, 42090, Tu¨rkiye.
[3]Department of Mechanical Engineering, Gazi University, Ankara, 06570, Tu¨rkiye.

*Corresponding author(s). E-mail(s): mahmut.kocagil@erzurum.edu.tr;
Contributing authors: ehcopur@erbakan.edu.tr; msalamci@gazi.edu.tr;

ARTICLE IN PRESS

Abstract

This paper proposes a direct Model Reference Adaptive Control (MRAC) architecture integrating a nonlinear reference model for a class of MIMO nonlinear systems with parameter uncertainty. The proposed Lyapunov-based adaptive rule makes the MRAC architecture favourable for a class of nonlinear MIMO systems in the presence of uncertainties. ~~This generic and systematic~~ The systematic method also allows nonlinear MRAC architecture to be built as flexible as possible, making it more practical and straightforward to apply in real-time for nonlinear uncertain systems. To demonstrate the effectiveness of the proposed MRAC rule, it is compared against classical MRAC approach through simulations and experiments performed on 3 DoF laboratory helicopter. In addition, the robustness ~~property~~ analysis of the proposed MRAC approach is also ~~investigated~~ performed through Monte Carlo simulations.

Keywords: MRAC, SDRE, Nonlinear Control, Nonlinear Reference Model, Real-Time Systems

1 Introduction

Model Reference Adaptive Control (MRAC) is one of the main approaches in adaptive control design [1–3]. A classical MRAC structure is usually comprised of a reference model, plant, controller, and adaptation mechanism. In this configuration, a stable

ARTICLE IN PRESS

reference model is first built or selected to produce a desired response to a given input (command). Then, a controller and an adaptive law used to update control parameters are designed to force the states of the uncertain plant to track the reference model trajectories. Therefore, MRAC can be defined as a control system that can accommodate the system uncertainty by updating the control law online with the information from the plant and reference models [4]. This ability of MRAC approach is its real power.

The main issue in MRAC design that should be taken into account is the structure of the reference model. The reason is that a reference model serves to shape the asymptotic behaviour of the uncertain plant. In the years when processing power (capacity) was much less than today, researchers generally preferred to design and implement control methods based on linear control theory. This approach has also been advocated by researchers working on the MRAC method. In the vast majority of MRAC schemes, a stable, completely known and linear model is usually utilised as a reference model [5–10] because a linear reference model can be effortlessly designed to meet the desired transient and steady-state response characteristics. However, this common approach may limit the effectiveness of the MRAC approach when attempting to solve the tracking control problem of the plant with strong non-linearities. Since a linear reference model may not be capable of representing the dominant dynamics critical for nonlinear behaviour of plants, it may only provide the asymptotic behaviour of the uncertain plant in a narrow range [11]. In addition, the MRAC architecture with a linear reference model may exhibit a poor tracking performance, and thereby is not really suitable for practical applications [12].

To address these limitations and capture the complex dynamics of plants, the switched systems framework has emerged as a basis for adaptive control design. Rather than relying on a single linear reference model, representing the plant as a family of switched linear subsystems governed by a switching signal enables a more flexible approximation of nonlinear behavior. Recent advances in this domain have improved the stability, robustness, and performance bounds of adaptive control for switched systems with parametric uncertainties. For instance, novel stability analysis methods using differential and algebraic Lyapunov equations have been developed to guarantee asymptotic stability under specific dwell-time constraints, ensuring a decreasing Lyapunov function both within and at switching instants [13]. To broaden the practical applicability of these constraints, recent approaches have focused on optimizing flexible dwell-time configurations and establishing tighter robustness bounds against unmodelled dynamics [14]. Furthermore, to enhance transient and steadystate performance in the presence of external disturbances, advanced parameter estimation techniques have been integrated into switched adaptive architectures [15]. Beyond continuous-time formulations, these methodologies have also been successfully extended to discrete-time switched systems, offering generalized frameworks that robustly handle structural switching alongside parametric variations [16]. Consequently, embedding a switched systems perspective into control architectures can overcome the narrow operational range of conventional linear reference models.

ARTICLE IN PRESS

On the other hand, thanks to advancements in control theory and technology, nonlinear controllers have been utilized for many years in real-time control applications of many different industries, such as aerospace and automotive. In recent years, many researches have focused on developing more advanced nonlinear control approaches since it has been proved that they are able to provide more promising control performance and meet control requirements more successfully than their linear counterparts. Among these control approaches, State-Dependent Riccati Equation (SDRE)-based controller is one of the widely-used nonlinear control approaches due to its easy implementability and design flexibility. However, it is still impossible to derive a highly accurate nonlinear mathematical model for the design of model-based nonlinear controllers such as SDRE or nonlinear Sliding Mode Controller, which limits the performance of nonlinear controllers in some cases, especially when the plant dynamics is completely unknown. To address the control problems with unknown plant dynamics and profit from the power of the nonlinear control theory allowing to design a stable nonlinear model easily, a new approach has recently emerged in MRAC theory in which a nonlinear reference model is employed rather than a linear reference model. It is supposed that a plant can track more successfully state trajectories generated by a stable nonlinear reference model than a stable linear reference model in MRAC architecture. The underlying reason of this is the fact that nonlinear models are more reliable and accurate for describing the dominant dynamics, mainly due to complex nonlinearities, than linear ones. Therefore, the use of a nonlinear reference model can generate more appropriate trajectories that can be more accurately tracked by unknown systems. The growing number of real-time applications of SDRE controllers has led the practitioners to use stabilized nonlinear dynamics by the SDRE as a nonlinear reference model in the MRAC instead of a linear reference model. Obviously, using a nonlinear reference model requires solving SDRE in real-time, which poses its own difficulties and complexities. However, there are many algorithms for solving SDRE in real-time applications. Some of these algorithms have been reviewed previously by Copur et al, in which a new algorithm has been also introduced to deal with the difficulty and complexity in solving SDRE [17]. These issues have been partially addressed in recent studies [12, 18–23], however the capabilities of having a nonlinear reference model have not been rigorously studied in detail.

Additionally, the performance of MRAC approach is adversely affected by the modelling accuracy and the degree of uncertainty. To overcome this drawback, different techniques have been developed, such as σ-modification and e-modification techniques [24–29]. However, for the nonlinear MRAC approach with a nonlinear reference model, to the best of the authors knowledge, a robustness analysis has not been performed yet. Therefore, it is important to investigate the robustness ~~property~~ of the nonlinear MRAC approach with a nonlinear reference model against the parameter uncertainties in the plant dynamics.

Considering the challenges mentioned above, this study aims twofold:

ARTICLE IN PRESS

1. To improve the control performance of the conventional direct MRAC scheme, a nonlinear reference model is utilized whose dynamics is in line with the nonlinear behavior of the plant. In previous studies by the authors [20, 21], an infinite-time Lyapunov equation was used to prove the stability of the nonlinear reference model for MRAC. However, the infinite-time Lyapunov equation may be insufficient for the stability analysis of nonlinear state-dependent systems due to the requirement for a state-dependent form of the algebraic Riccati equation. Therefore, in the Lyapunov stability analysis, the derivative of the Lyapunov candidate function includes the time derivative of the solution of the Lyapunov equation, which can destabilize the system if the states change rapidly. The stability of the proposed approach is proven by using Lyapunov stability theory, and from the proof, a state-dependent adaptation gain matrix is derived, which is simultaneously updated by solving a differential Lyapunov equation in a finite time. The simulation and experimental results show that the proposed approach enables the plant states to track the reference trajectory, i.e., the response of the nonlinear reference model to a reference input, in a more precise and agile manner than the MRAC approach with a linear reference model.
2. Unlike the authors' previous studies [20, 21], this study proposes a robustness analysis to examine the control performance of the proposed approach against parametric uncertainties in the plant dynamics, without introducing an additional robust mechanism into the adaptation rule. To perform a robustness analysis for the proposed MRAC approach, a nonlinear plant model with bounded uncertain parameters is considered. To evaluate the robustness of the proposed MRAC approach, it is compared with the MRAC approach with a linear reference model in Monte Carlo simulations. A set of simulations is performed by varying the state-dependent plant parameters randomly, and the simulation results demonstrate that the proposed approach ~~can improve the robustness against the uncertain parameters compared to MRAC approach with the linear reference model.~~ is able to reduce the adverse effects of the parametric uncertainties in the plant dynamics than the classical MRAC with a linear reference model. Here, it needs to be clarified that this study does not aim to design a robust MRAC approach. Rather, it demonstrates that the tracking performance of the presence of bounded parametric uncertainties without an additional robustness mechanism.

This paper is organized as follows: SDRE and SDRE-based MRAC designs for nonlinear systems are presented in Section2, respectively. Section3.1 presents a simulation study comparing the performance of direct MRAC approaches with linear and nonlinear reference models in controlling a second-order fictitious nonlinear system. In Section3.2 the nonlinear and linearised mathematical models of the laboratory helicopter are given and then experimental results are also discussed. The conclusion is given in Section4.

ARTICLE IN PRESS

2 Methods

This section explains how to design a state-dependent MRAC approach using a nonlinear reference model. The classical MRAC theory relies on manipulating the state trajectories of the uncertain plant so that they are forced to follow the state trajectories of the linear reference model. This control approach is realized by an adaptive control law designed in a manner to adapt itself to the uncertain plant dynamics so as to nullify the error between the plant and the reference model states.

A nonlinear reference model can mathematically express at least the dominant nonlinear characteristics of the plant dynamics and therefore is more reasonably capable of mimicking the behavior of the unknown plant than a linear reference model. This important feature of the nonlinear reference model allows the adaptive control law in the state-dependent MRAC approach to drive the plant state trajectories towards the state trajectories of the nonlinear reference model more successfully than those of the linear reference model. However, MRAC approach requires a reference model stabilized in a desired fashion so that its state trajectories can follow the pre-defined command trajectories closely.

Nonlinear systems can be stabilized using many different controller design methods. Amongst them, SDRE approach that serves as a suboptimal control method is one of the widely used control methods for nonlinear systems. In the control community, it is considered as the extension of LQR method to nonlinear systems. In the following subsection, SDRE approach will be briefly introduced to design a stable nonlinear reference model.

2.1 Controller Design for Nonlinear Reference Model: SDRE Approach

Consider a nonlinear time-invariant control-affine reference model in the following general form

$$\dot{x}_m = f_m(x_m) + B_m(x_m)u_m \tag{1}$$

where $x_m(t) \in \mathrm{D}$ denotes the reference model states in a bounded open set $\mathrm{D} \subseteq \mathrm{R}^n$, $u_m(t) \in \mathrm{R}^m, (1 \le m \le n)$ is the control vector and $B_m(x_m) = 0 \in \mathrm{R}^{n\times m}$ is a completely known input matrix of the model with a completely known smooth vector field $f_m(x_m)$. In addition, the function $f_m(x_m)$ of the nonlinear system (1) can be represented in an equivalent structure under the following assumption.

Assumption 1 Given a bounded open set $\mathrm{D} \subseteq \mathrm{R}^n$, $x_m = 0 \in \mathrm{D} \subset \mathrm{R}^n$ is an equilibrium point when $f_m(0) = 0$ with $u_m(t) = 0$ and $f_m(x_m) : \mathrm{D} \to \mathrm{R}^n$ is a continuously differentiable vector-valued function in region D (i.e. $f_m(x_m)$ satisfies locally Lipschitz condition with zero equilibrium point).

Then $f_m(x_m)$ can be parametrised in a state-dependent coefficient (SDC) form

ARTICLE IN PRESS

$$f_m(x_m) = A_m(x_m)x_m \tag{2}$$

where $A_m(x_m) : \mathsf{D} \rightarrow \mathsf{R}^{n\times n}$. Assumption 1 guarantees the existence of the SDC parametrisation (2) and for multi-variable case when $n > 1$, this parametrisation is not unique [30]. Finally, the parametrisation of $f_m(x_m)$ yields

$$\dot{x}_m = A_m(x_m)x_m + B_m(x_m)u_m,\ x_m(t_0) = x_{m0} \tag{3}$$

To ensure the convergence of x_m to the equilibrium point in a finite time horizon starting from t_0 to t_f, the following state-feedback control law can be applied

$$u_m = -K_m(x_m)x_m \tag{4}$$

where $K_m(x_m) \in \mathsf{R}^{m\times n}$ is defined as feedback gain matrix. SDRE approach minimizes a quadratic performance index (i.e. cost function) given by

$$J=\frac{1}{2}\{x_m^\top S x_m+\int_{t_0}^{t_f}[x_m^\top Q_m(x_m)x_m+u_m^\top R_m(x_m)u_m]dt\} \tag{5}$$

where $S \in \mathsf{R}^{n\times n}$ is a non-negative definite symmetric matrix, $Q_m(x_m) \in \mathsf{R}^{n\times n}$ is a state weighting matrix and $R_m(x_m) \in \mathsf{R}^{m\times m}$ is an input weighting matrix. As in most cases, the matrix S is however selected to be a zero matrix. For the state-dependent cases, to obtain the minimum value of the quadratic performance index (5)

$$J^*=\frac{1}{2}\min_{u_m}\left[\int_{t_0}^{t_f}\{x_m^\top Q_m(x_m)x_m+u_m^\top R_m(x_m)u_m\}\,dt\right] \tag{6}$$

the suboptimal control law can be obtained in the form

$$u_m = -R_m^{-1}(x_m)B_m^\top(x_m)P_m(x_m)x_m \tag{7}$$

where $P_m(x_m) \in \mathsf{R}^{n\times n}$ is the positive definite matrix and is the solution of the following state-dependent differential Riccati equation (SDDRE) given by

$$-\dot{P}_m(x_m) = P_m(x_m)A_m(x_m) + A_m^\top(x_m)P_m(x_m) - P_m(x_m)B_m(x_m)R_m^{-1}(x_m) \times B_m^\top(x_m)P_m(x_m) + Q_m(x_m) \tag{8}$$

Remark 1 SDDRE (8) can be derived by using the necessary conditions for optimality ([31, See, Pontryagin's minimum principle]). The sub-optimality property of infinite-time horizon

ARTICLE IN PRESS

SDRE approach has been given in [32, See Proof of the Theorem 4]. Therefore, the suboptimality property of the finite-time horizon SDRE approach can be proven by following the same steps, except that $\dot{P}_m(x_m)$ must be replaced by Eq. (8).

The solution of the SDDRE can be guaranteed for all $x_m(t) \in \mathrm{D}$ if the following conditions are both satisfied [32].

Condition 1 $A_m(\cdot)$, $B_m(\cdot)$, $Q_m(\cdot)$ and $R_m(\cdot)$ are $C^1(\mathrm{R}^n)$ matrix-valued functions. Moreover, $Q_m(x_m)$ and $R_m(x_m)$ are non-negative and positive definite matrices, respectively.

Condition 2 The SDC matrix pairs $\{A_m(x_m),B_m(x_m)\}$ and $\{A_m(x_m),Q^{0.5}_m(x_m)\}$ are stabilizable and detectable, respectively for $\forall x_m \in \mathrm{D}$.

Remark 2 The non-uniqueness of SDC parametrisation provides a great design flexibility to improve controller performance, prevent singularities or loss of controllability. This means that SDC parametrisation can be arbitrarily made to obtain a suitable nonlinear structure (3) that satisfies Condition 2 [33, See Proposition 1].

Thus, the suboptimal control law (7), which involves the solution of Riccati equation (8), can be applied to Eq. (3) and it yields the closed-loop system

$$\dot{x}_m = A_{mcl}(x_m)x_m \tag{9}$$

where $A_{mcl}(x_m) := A_m(x_m) - B_m(x_m)K_m(x_m)$. From Eqs. (4) and (7), the feedback gain matrix $K_m(x_m)$ becomes

$$K_m(x_m) = R_m^{-1}(x_m)B_m^{\top}(x_m)P_m(x_m)$$

The following theorem ensures the local asymptotic stability of the closed-loop system.

Theorem 1 *(See [30, 34–36]) Considering Conditions (1) and (2), the output of the state dependent nonlinear system (1) can be stabilized by using the proposed state feedback law (7) where $P_m(x_m)$ is the unique solution of the SDDRE (8) on the finite-time horizon.*

In the section that follows, the adaptive control law will be introduced to drive the state trajectories of the unknown nonlinear plant towards the state trajectory of the closed-loop nonlinear reference model (9).

2.1.1 Modified Adaptive Control Law Design Considering the Nonlinear Reference Model

Consider a nonlinear state dependent control-affine plant in the form

ARTICLE IN PRESS

$$\dot{x}_p = f_p(x_p) + B_p(x_p)u_p \tag{10}$$

Under the Assumption 1, any nonlinear plant model can be parametrised in the structure similar to $\dot{x} = A(x)x+B(x)u$ [33]. Since this assumption is also compatible with the nonlinear plant model (10), SDC parametrisation yields $f_p(x_p) = A_p(x_p)x_p$. Then the plant (10) can be rewritten as

$$\dot{x}_p = A_p(x_p)x_p + B_p(x_p)u_p,\ x_p(0) = x_{p0} \tag{11}$$

where $A_p(x_p) : \mathsf{D} \rightarrow \mathsf{R}^{n\times n}$ and $B_p(x_p) : \mathsf{D} \rightarrow \mathsf{R}^{n\times m}$ ($B_p(x_p) \neq 0\ \forall x_p$) are assumed possibly unknown state-dependent matrices. Here, a proper adaptive control input $u_p \in \mathbb{R}^m, (1 \leq m \leq n)$

$$u_p = -K_p(x_p,x_m)x_p(t) \tag{12}$$

can be derived to drive the error state $e(t)$, i.e. $e(t) = x_p(t) - x_m(t)$, to zero asymptotically. If $A_p(x_p)$ and $B_p(x_p)$ were completely known, u_p could become

$$u_p = -K_p^*(x_p, x_m)x_p \tag{13}$$

with the ideal state-dependent feedback gain $K_p^*(x_p, x_m) \in \mathbb{R}^{m\times n}$ that satisfies the perfect matching condition

$$A_p(x_p) - B_p(x_p)K_p^*(x_p, x_m) = A_{m_{cl}}(x_m) \tag{14}$$

Assumption 2 ~~There exists an ideal feedback gain $K_p^*(x_p,x_m)$ with the known SDC matrix pairs $\{A_p(x_p),B_p(x_p)\}$ for $\forall x_p \in \mathsf{D}$.~~ The nonlinear plant is represented in a state-dependent coefficient (SDC) form. Although the state-dependent matrices $A_p(x_p)$ and $B_p(x_p)$ are structurally known, it is assumed that there exist ideal state-dependent feedback gain $K_p^*(x_p,x_m)$, such that the perfect matching conditions $A_p(x_p) - B_p(x_p)K_p^*(x_p, x_m) = A_{m_{cl}}$ hold for all $x_p \in \mathsf{D}$ if $A_p(x_p)$ and $B_p(x_p)$ are fully known.

According to Theorem1, the eigenvalues of $A_{mcl}(x_m)$ satisfies $\mathrm{Re}[\lambda_{i=1,\ldots,n}(A_{mcl}(x_m))] < 0$, thereby $e(t) \rightarrow 0$ when $t \rightarrow \infty$. This error evolution also leads to the asymptotic convergence of the plant states $x_p(t)$ to the reference states $x_m(t)$. However, with unknown system matrices, the determination of the feedback gain becomes more difficult since, for the case with known matrices, the ideal feedback gain can be easily obtained by a straightforward matrix operation using (14). To cope with the issue ~~arisen~~ arising from the unknown matrices, an estimation approach can be used to predict the feedback gain $K_p(x_p,x_m)$. This approach enables $K_p(x_p,x_m)$ to adapt itself over time to compensate for variations in the nonlinear dynamics of the plant.

ARTICLE IN PRESS

Before deriving the adaptation law for $K_p(x_p,x_m)$, an important assumption is given as follows:

Assumption 3 ~~There exist a positive definite matrix $G \in \mathbb{R}^{m\times m}$, such that the estimation of the input matrix, $\check{B}_p(x_p) = B_p(x_p)G$ is known.~~ There exists a triangular matrix with non-zero diagonal entries $G \in \mathbb{R}^{m\times m}$, such that the estimation of the input matrix, $\check{B}_p(x_p) = B_p(x_p)G$ is known.

Remark 3 During flight operations, flight controllers must be robust against uncertainties, especially due to actuator faults to improve safety and security. In adaptive flight controller design, Assumption 3 has been widely used to describe a faulty scenario where loss of effectiveness and reversal in control input occur [37, 38].

The following theorems are introduced to derive the adaptation law to compute $K_p(x_p,x_m)$.

Theorem 2 *(See [39], Section 4.1.1) Given $x_m,x_p \in \mathbb{D}$, there exists a unique positive definite matrix $P_{ad}(x_p,x_m) : \mathbb{R}^{2n} \to \mathbb{R}^{n\times n}$ satisfying the Lyapunov equation*

$$-\dot{P}_{ad}(x_p,x_m) = P_{ad}(x_p,x_m)A_{m_{cl}}(x_m) + A^{\top}_{m_{cl}}(x_m)P_{ad}(x_p,x_m) + Q_{ad}(x_p) \tag{15}$$

$$^{\top} P_{ad}(x_{p0},x_{m0}) =$$

$$P_{ad0} = P_{ad0}$$

where $Q_{ad}(x_p) \in \mathbb{R}^{n\times n}$ is an arbitrary positive definite matrix-valued function if and only if $A_{m_{cl}}(x_m)$ is a Hurwitz matrix for any given positive definite matrix $Q_{ad}(x_p)$.

Theorem 3 *Let $\tilde{K}(x_p,x_m) \triangleq K_p(x_p,x_m) - K_p^*(x_p,x_m)$ and $e \triangleq x_p - x_m$. If $\dot{\tilde{K}}(x_p,x_m) = \check{B}_p^{\top}(x_p)P_{ad}(x_p,x_m)ex^{\top}_p\Gamma$, then $x_p(t)$ and $e(t)$ are bounded and $x_p(t)$ converges to $x_m(t)$ as $t \to \infty$, i.e. $e(t) \to 0$ as $t \to \infty$.*

Proof 1 *Let*

$$e \triangleq x_p - x_m \tag{16}$$

be the tracking error. Substituting (12) into (10) yields

$$\dot{x}_p = A_p(x_p)x_p + B_p(x_p)(-K_p(x_p,x_m)x_p) \tag{17}$$

Considering (14) and definition of $K_e(\cdot)$, Eq. (17) can be rewritten as

$$\dot{x}_p = \left(A_{m_{cl}}(x_m) + B_p(x_p)K_p^*(x_p,x_m)\right)x_p - B_p(x_p)\left\{(\tilde{K}(x_p,x_m) + K_p^*(x_p,x_m))\right\}x_p$$

$$\dot{x}_p = A_{m_{cl}}(x_m)x_p(t) - B_p(x_p)\tilde{K}(x_p,x_m)x_p \tag{18}$$

Substituting (16) into (18) yields

ARTICLE IN PRESS

ARTICLE IN PRESS

$$\dot{x}_p = A_{mcl}(x_m)\{e + x_m\} - B_p(x_p)\tilde{K}(x_p,x_m)x_p$$

$$= A_{mcl}(x_m)e + A_{mcl}(x_m)x_m - B_p(x_p)\tilde{K}(x_p,x_m)x_p$$

and with (9), it becomes

$$\dot{x}_p = A_{mcl}(x_m)e + \dot{x}_m - B_p(x_p)\tilde{K}(x_p,x_m)x_p$$

$$\dot{x}_p - \dot{x}_m = A_{mcl}(x_m)e - B_p(x_p)\tilde{K}(x_p,x_m)x_p$$

Then, the error dynamics is derived

$$\dot{e}(t) = A_{mcl}(x_m)e(t) - B_p(x_p)\tilde{K}(x_p,x_m)x_p(t) \tag{19}$$

and with Assumption (3), it becomes

$$\dot{e} = A_{mcl}(x_m)e(t) - \check{B}_p(x_p)G^{-1}\tilde{K}(x_p,x_m)x_p$$

$$e(0) = x_{p0} - x_{m0}$$

Now consider the following positive definite Lyapunov function candidate

$$V(e(t),\tilde{K}(\cdot)) = e^\top P_{ad}(x_p,x_m)e + tr(G^{-1}\tilde{K}(x_p,x_m)\Gamma^{-1}\tilde{K}^\top(x_p,x_m)) \tag{20}$$

The time derivative of $V(e(t),\tilde{K}(x_p,x_m))$ is evaluated as follows:

$$\dot{V}(e(t),\tilde{K}(\cdot)) = \dot{e}^\top P_{ad}(x_p,x_m)e(t) + e^\top\{\dot{P}_{ad}(x_p,x_m)e(t) + P_{ad}(x_p,x_m)\dot{e}\}$$

$$+ tr\{G^{-1}\dot{\tilde{K}}(x_p,x_m)\Gamma^{-1}\tilde{K}^\top(x_p,x_m) + G^{-1}\tilde{K}(x_p,x_m)\Gamma^{-1}\dot{\tilde{K}}^\top(x_p,x_m)\}$$

$$\dot{V}(\cdot,\cdot) = \{e^\top A^\top_{mcl}(x_m) - x^\top_p\tilde{K}^\top(x_p,x_m)G^{-1}\check{B}^\top_p(x_p)\}P_{ad}(x_p,x_m)e$$

$$+ e^\top\{\dot{P}_{ad}(x_p,x_m)e + P_{ad}(x_p,x_m)[A_{mcl}(x_m)e - \check{B}_p(x_p)G^{-1}\tilde{K}(x_p,x_m)x_p]\}$$

$$+ 2tr(G^{-1}\dot{\tilde{K}}(x_p,x_m)\Gamma^{-1}\tilde{K}^\top(x_p,x_m))$$

$$\dot{V}(\cdot,\cdot) = e^\top A^\top_{mcl}(x_m)P_{ad}(x_p,x_m)e - x^\top_p\tilde{K}^\top(x_p,x_m)G^{-1}\check{B}^\top_p(x_p)P_{ad}(x_p,x_m)e$$

$$+ e^\top\dot{P}_{ad}(x_p,x_m)e + e^\top P_{ad}(x_p,x_m)A_{mcl}(x_m)e$$

$$- e^\top P_{ad}(x_p,x_m)\check{B}_p(x_p)G^{-1}\tilde{K}(x_p,x_m)x_p + 2tr(G^{-1}\dot{\tilde{K}}(x_p,x_m)\Gamma^{-1}\tilde{K}^\top(x_p,x_m))$$

$$\dot{V}(\cdot,\cdot) = e^\top\{A^\top_{mcl}(x_m)P_{ad}(x_p,x_m) + \dot{P}_{ad}(x_p,x_m) + P_{ad}(x_p,x_m)A_{mcl}(x_m)\}e$$

$$- x^\top_p\tilde{K}^\top(x_p,x_m)G^{-1}\check{B}^\top_p(x_p)P_{ad}(x_p,x_m)e - e^\top P_{ad}(x_p,x_m)\check{B}_p(x_p)G^{-1}\tilde{K}(x_p,x_m)x_p$$

$$+ 2tr(G^{-1}\dot{\tilde{K}}(x_p,x_m)\Gamma^{-1}\tilde{K}^\top(x_p,x_m))$$

$$\dot{V}(\cdot,\cdot) = e^\top\{-Q_{ad}(x_p)\}e - 2e^\top P_{ad}(x_p,x_m)\check{B}_p(x_p)G^{-1}\tilde{K}(x_p,x_m)x_p$$

ARTICLE IN PRESS

ARTICLE IN PRESS

$$+ 2tr(G^{-1}\dot{\tilde{K}}(x_p,x_m)\Gamma^{-1}\tilde{K}^{\top}(x_p,x_m))$$

$$\dot{V}(\cdot,\cdot) = e^{\top}\{-Q_{ad}(x_p)\}e - 2tr\{e^{\top}P_{ad}(x_p,x_m)\check{B}_p(x_p)G^{-1}\tilde{K}(x_p,x_m)x_p\}$$

$$+ 2tr\{G^{-1}\dot{\tilde{K}}(x_p,x_m)\Gamma^{-1}\tilde{K}^{\top}(x_p,x_m)\}$$

Using some trace properties, it follows that

$$\dot{V}(\cdot,\cdot) = -e^{\top}Q_{ad}(x_p)e + 2tr\{G^{-1}[\dot{\tilde{K}}(x_p,x_m)\Gamma^{-1} - \check{B}_p^{\top}(x_p)P_{ad}(x_p,x_m)ex_p^{\top}]\tilde{K}^{\top}(x_p,x_m)\}$$

Since $\dot{\tilde{K}}(x_p,x_m) = \check{B}_p^{\top}(x_p)P_{ad}(x_p,x_m)ex_p^{\top}\Gamma$, *then* $\dot{V}(\cdot,\cdot)$ *takes the form of*

$$\dot{V}(e(t),\tilde{K}(\cdot)) = -e^{\top}(t)Q_{ad}(x_p)e(t) \leq -\lambda_{min}(Q_{ad}(x_p))\|e(t)\|_2^2 \leq 0 \qquad (21)$$

where $\lambda_{min}(Q_{ad}(x_p))$ *is the minimum eigenvalue of the symmetric* $Q_{ad}(x_p)$ *matrix.* $Q_{ad}(x_p)$, $\tilde{K}(x_p,x_m)$ *and* e *are bounded since* $\dot{V}(e(t),\tilde{K}(\cdot)) \leq 0$. *Therefore,* $\dot{e}$ *and* $\dot{Q}_{ad}(x_p)$ *are also bounded. These boundedness properties imply that*

$$\ddot{V}(e,\tilde{K}(\cdot)) = -\dot{e}^{\top}Q_{ad}(x_p)e - e^{\top}Q_{ad}(x_p)\dot{e} - e^{\top}\dot{Q}_{ad}(x_p)e$$

is bounded and makes $\dot{V}(e(t),\tilde{K}(\cdot))$ *uniformly continuous. Then, using Barbalat's Lemma, it is stated that* $\dot{V}(e(t),\tilde{K}(\cdot)) \to 0$, *and hence* $e(t) \to 0$ *as* $t \to \infty$. □

It should be noted that continuous measurement of the states may not be practical because of discretized implementation of the state feedback control mechanism. As proposed in all SDRE based control algorithms (see [33, 40] and the references therein), the dynamics of the system is frozen for an instant in time at which the system is considered to be time invariant. Due to this fact, the following assumption will be used in practice.

Assumption 4 Time derivatives of $\tilde{K}(\cdot)$ and $K_p(\cdot)$ are equal at each instant in time at which the system dynamics are frozen and the system is considered to be time invariant.

Remark 4 Assumption 4 predicts $K_p(\cdot)$ from $\tilde{K}(\cdot)$. This assumption does not necessarily mean that $K_p(\cdot) = \tilde{K}(\cdot)$, however $K_p(\cdot)$ and $\tilde{K}(\cdot)$ do have the same slope at each instant in time, as shown in Figure 1. As a consequence, $\dot{K}_p^*(x_p,x_m)$ vanishes at these instants.

ARTICLE IN PRESS

ARTICLE IN PRESS

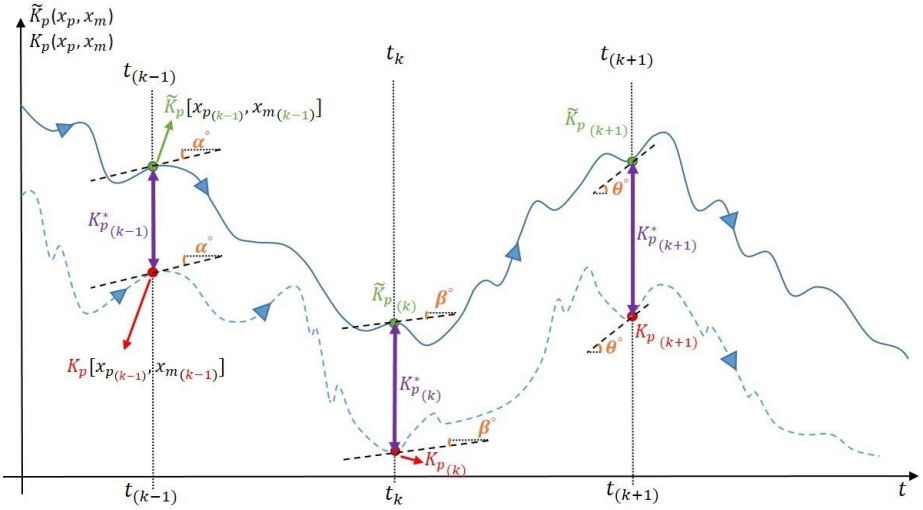


Fig. 1: Schematic diagram of adaptive gain evolution

Under Assumption 4, $\dot{\widetilde{K}}_p(x_p,x_m) = \dot{K}_p(x_p,x_m)$ at each instant in time. Thus, to estimate $K_p(\cdot)$, the following adaptive law is used,

$$\dot{K}_p(x_p, x_m) = \check{B}_p^\top(x_p) P_{ad}(x_p, x_m) e(t) x_p^\top(t) \Gamma \tag{22}$$

where the differential equation is solved with the initial condition, $K_{p0} \in \mathbb{R}^{m \times n}$ which is an initial estimation of $K_p(x_p,x_m)$. Additionally, $\Gamma \in \mathbb{R}^{n \times n}_{>0}$ is the learning rate and is used to increase the rate at which the error $e(t)$ ~~convergences~~ converges to zero.

Remark 5 This study introduces a condition, which is similar to that in the previous study [22], to ensure the convergence of the error. The main difference is that the condition proposed here is provided by solving a differential Lyapunov equation to cover continuity of the process which is more feasible for real-time applications.

Implementation of SDRE based MRAC approach is explained in the following subsection.

2.1.2 Implementation of SDRE based MRAC Approach

In general, for multivariable cases, the solution of SDDRE (8) is obtained through on-line numerical computation as in this study. The real-time implementation of the proposed control approach is based on a sampled-data form of the equations (7)-(9) in continuous time. In so doing, the SDC matrices $A_m(x_m)$ and $B_m(x_m)$ are computed for the

ARTICLE IN PRESS

reference state vector $x_m(t_k)$ at each time instant t_k to produce the following pointwise matrices

$$A_m(x_m(t_k)) = A_m(x_{mk}) = A_{mk}\, B_m(x_m(t_k)) = B_m(x_{mk}) = B_{mk}$$

Similarly, the weighting matrices $Q_m(x_{mk})$ and $R_m(x_{mk})$ are also computed at each time instant t_k as $Q_m(x_{mk}) = Q_{mk}$ and $R_m(x_{mk}) = R_{mk}$.

The existence of a set of sampling times for which the closed-loop state-feedback regulator using SDRE approach with sampled-data form is asymptotically stable is proven in [41], under Condition 1 and Condition 2. The theoretical study [41] provides substantial insights into the choice of the proper sampling interval, i.e. $\Delta t = t_{k+1} - t_k$ and remarks an interaction between the sampling time Δt, the reference system matrices ($A_m(\cdot)$ and $B_m(\cdot)$), the state weighting matrix $Q_m(\cdot)$ and the Riccati solution $P_m(\cdot)$. It is suggested [41] that Δt must be selected to be small enough to produce small rate of change in $A_m(\cdot)$, $B_m(\cdot)$ and $P_m(\cdot)$. According to [33], although several constraints exist, in general they do not pose a problem as they all require a small selection of sampling time. In addition, the stability of the state-feedback regulators may be increased by choosing relatively larger $Q_m(x_{mk})$ at the expense of higher control need leading to compromise optimality.

In the implementation procedure of SDRE, A_{mclk} is determined as a pointwise Hurwitz in the region of D at each time instant t_k and specified as $\mathrm{Re}[\lambda_i(A_{mclk})] < 0, \forall x_{mk} \in \mathrm{D}$ eventually. Thus, x_{mk} is converged asymptotically to the local stable equilibrium points through the state-feedback control law u_{mk}.

In MRAC approach, the sampled-data implementation is also possible. For the state-dependent and possibly unknown plant whose stabilization is provided by the reference model, the issue can be similarly eliminated by choosing a small predetermined sampling interval size. Thus, the adaptation mechanism and control law computations ($\dot{K}_{pk}$ and u_{pk}, respectively) become possible through the defined tracking error state, e_k and the solution of differential Lyapunov equation, P_{adk}. Fig. 2 illustrates how the adaptation law works with the sampled data forms of the reference and plant models given by a general linear system $\dot{x}_{lk} = A_{lk}x_{lk} + B_{lk}u_{lk}$ where $l = p,r$. With the frozen system matrices (A_{lk},B_{lk}) at t_k, the state-dependent feedback gain $K_p^*(x_m,x_p)$ becomes constant within the time interval between t_k and t_{k+1} and therefore the derivative of constant K_p^* vanishes. This approach enables to update the adaptive law

(22) with the frozen system matrices (A_{lk},B_{lk}) at t_k and implement Theorem 3 in the digital computations.

ARTICLE IN PRESS

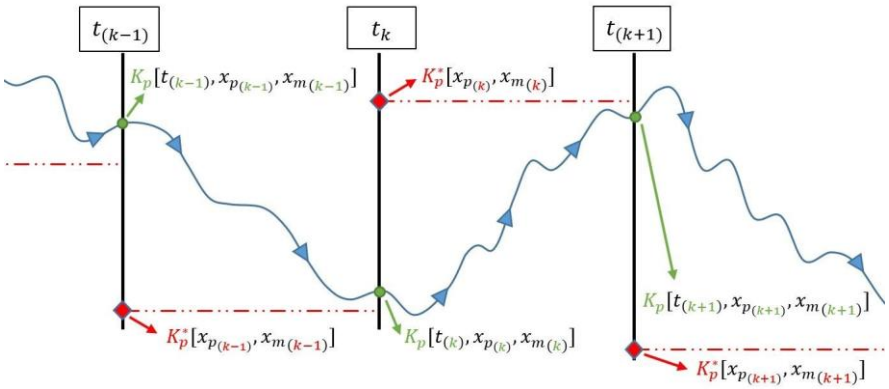


Fig. 2: Implementation process of K_p in the proposed MRAC approach

3 Results and Discussion

3.1 Simulation Study

To evaluate the effectiveness of the proposed MRAC approach, a comparative study is conducted in simulations by considering three different cases. These cases are explained in the following subsections in details. Then, the robustness analysis of MRAC approach against the uncertainties in the parameters of the nonlinear plant ~~(NLP)~~ is also ~~investigated.~~ performed. In the robustness analysis, the responses of uncertain plants to different types of test commands are compared when the MRAC method with a nonlinear reference model ~~(NLRM)~~ and a linear reference model ~~(LRM)~~ is applied. To enhance readability for the reader, abbreviations designating the linearity and classifications of the dynamic systems utilized throughout the manuscript are provided in parentheses: Linear (L), Linear reference (LR), Linear reference model (LRM), Linear plant (LP), Nonlinear (NL), Nonlinear reference (NLR), Nonlinear reference model (NLRM), Nonlinear plant (NLP).

3.1.1 NLR and NLP Models to be used for Simulation Studies

For the simulation study, the following second-order fictitious NLRM [42] is employed.

$$\begin{aligned} \dot{x}_{m1} &= x_{m2} \\ \dot{x}_{m2} &= -x_{m1}e_{xm1} + 0.5x_{2m2} + e_{xm1}u_m \end{aligned} \tag{23}$$

that can be also expressed in the following SDC form

$$\begin{bmatrix} \dot{x}_{m_1} \\ \dot{x}_{m_2} \end{bmatrix} = \begin{bmatrix} 0 & 1 \\ -e^{x_{m_1}} & 0.5x_{m_2} \end{bmatrix} \begin{bmatrix} x_{m_1} \\ x_{m_2} \end{bmatrix} + \begin{bmatrix} 0 \\ e^{x_{m_1}} \end{bmatrix} u_m \tag{24}$$

ARTICLE IN PRESS

to estimate the feedback gain $K_m(x_m)$ in the state-feedback control law (7) based on the differential Riccati equation. The controllability aspect of the NLRM (24) form is provided in Appendix B.

The NLP is generated by changing the constant coefficients (α_1,α_2 and α_3) in the state-dependent terms of the NLRM. Thus, the fabricated NLP is structurally similar to the NLRM, and is given by

$$\begin{aligned} \dot{x}_{p1} &= x_{p2} \\ \dot{x}_{p2} &= -\alpha_1 x_{p1} e_{xp1} + \alpha_2 x_{2p2} + \alpha_3 e_{xp1} u_p \end{aligned} \tag{25}$$

where $\alpha_1 = 3$,$\alpha_2 = 2$ and $\alpha_3 = 2$ are arbitrarily selected numbers, and it can be transformed into a SDC form

$$\begin{bmatrix} \dot{x}_{p_1} \\ \dot{x}_{p_2} \end{bmatrix} = \begin{bmatrix} 0 & 1 \\ -3e^{x_{p_1}} & 2x_{p_2} \end{bmatrix} \begin{bmatrix} x_{p_1} \\ x_{p_2} \end{bmatrix} + \begin{bmatrix} 0 \\ 2e^{x_{p_1}} \end{bmatrix} u_p \tag{26}$$

Once the state-space forms of the models are determined, a command-following controller can now be designed. The design procedure is applied for all the simulation studies. To perform the command-following task, the integral of the control-states is added to the system as a new state, thereby resulting in with an augmented system. The design procedure is clearly explained in Appendix A where $(\hat{\cdot})$ denotes the matrices and vectors of the augmented system, and $\bar{u}$ denotes the control input of the augmented system throughout the rest of the paper.

3.1.2 Comparison of the effectiveness for the proposed MRAC approach

A set of simulations is carried out in ~~MatLAB~~ –MATLAB/Simulink environment to investigate the control performance of the proposed MRAC approach. To verify the effectiveness of the proposed method, it is compared with three different MRAC methods. The implementation way of each method in the simulation studies is explained in an individual case given below. For a command-following design, the output vector $C^T = [1\ 0]$ is used to obtain the augmented systems. The controllability aspect of the augmented model of the NLRM (24) form is provided in Appendix C.

Case-I: In this case, the augmented systems of the nonlinear models (24) and (26) are respectively considered as the reference and plant models. Then SDRE method is applied to obtain the stable augmented closed-loop reference model $\hat{A}_{mcl}(\hat{x}_m)$. To estimate the feedback gain $\hat{K}_p(\hat{x}_p,\hat{x}_m)$ enabling the augmented NLP states to track the augmented NLRM states, the adaptive law is introduced as

$$\dot{\hat{K}}_p(\hat{x}_p, \hat{x}_m) = \check{\hat{B}}_p^{\top}(\hat{x}_p)\hat{P}_{ad}(\hat{x}_p, \hat{x}_m)\hat{e}(t)\hat{x}_p^{\top}(t)\,\hat{\Gamma} \tag{27}$$

ARTICLE IN PRESS

where the differential equation is solved with the initial condition, $\hat{K}_{p0} \in \mathrm{R}^{m\times(n+h)}$ which is an initial estimation of $\hat{K}_p(\hat{x}_p,\hat{x}_m)$ and $\check{\hat{B}}(\hat{x}_p)$ = [0 4exp($\hat{x}_{p1}$ − r) 0]$^\top$. The control architecture of Case-I is illustrated in Fig.3.

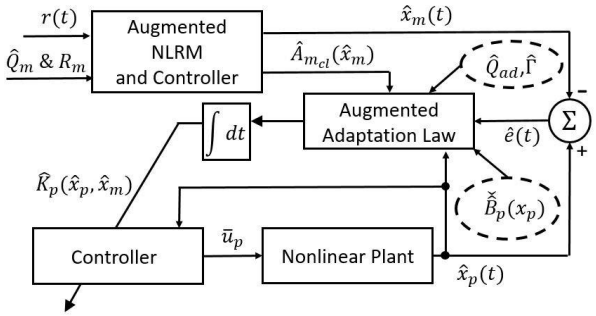


Fig. 3: Block Diagram for the Case-I

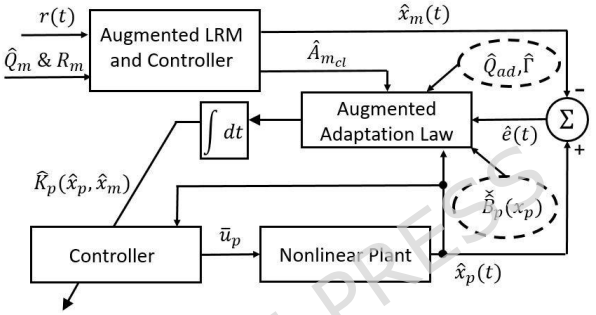


Fig. 4: Block Diagram for the Case-II

Case-II: In Case II, the nonlinear reference model is replaced with a linear reference model. The NLRM (23) is linearized around its equilibrium state and the resulting system becomes

$$\dot{x}_{m1} = x_{m2}$$

$$\dot{x}_{m2} = -x_{m1} + u_m \tag{28}$$

which is utilized as a linear reference model. Now, the classical LQR method can be applied to obtain the stable augmented closed-loop reference model $\hat{A}_{mcl}$. Using the augmented nonlinear plant model (NLPM), the following adaptive law can be derived to estimate the feedback gain $\hat{K}_p(\hat{x}_p,\hat{x}_m)$

$$\dot{\hat{K}}_p(\hat{x}_p,\hat{x}_m) = \check{\hat{B}}_p^\top(\hat{x}_p)\hat{P}_{ad}\hat{e}(t)\hat{x}_p^\top(t)\,\hat{\Gamma} \tag{29}$$

ARTICLE IN PRESS

ARTICLE IN PRESS

where B solution of the Riccati equation generated by the constant augmented system matrices

$\check{\hat{}}(\hat{x}_p) = [0\ 4\exp(\hat{x}_{p1}-r)\ 0]^\top$ and $\hat{P}_{ad}$ is the constant positive matrix that is the

($\hat{A}_m$ and $\hat{B}_m$) of the LRM (28). The control architecture of Case-II is depicted in Fig.4.

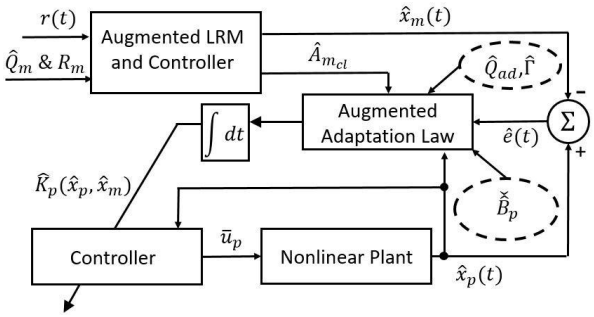


Fig. 5: Block Diagram for the Case-III

Case-III: In this case, the adaptive control input is computed by using the LRM (28) and linear plant model (LPM) but applied to the NLPM (26). The LPM is obtained by linearizing the NLPM (26) around the equilibrium point and is given as below:

$$\dot{x}_{p1} = x_{p2}$$

$$\dot{x}_{p2} = -3x_{p1} + 2u_p \tag{30}$$

To estimate the state-feedback gain, the adaptive law is derived as

$$\dot{\hat{K}}_p(\hat{x}_p, \hat{x}_m) = \hat{B}_p^\top \hat{P}_{ad}\hat{e}(t)\hat{x}_p^\top(t)\,\hat{\Gamma} \tag{31}$$

where $\check{B}_p = [0\ 4\ 0]^\top$ is the control input matrix of the augmented LPM and $\hat{x}_p(t)$ is the augmented state vector of the NLPM (26). Then, the following state-feedback adaptive control law is applied to the NLPM

$$\bar{u}_p = -\hat{K}_p(\hat{x}_p, \hat{x}_m)\hat{x}_p(t) \tag{32}$$

The control architecture of Case-III is given in Fig. 5.

3.1.3 Discussion on Results of Three Cases

For the simulation study, the initial conditions for the states and gain vectors, the weighting matrices, and the learning rate are, respectively, selected to be $x_{m0} = x_{p0} =$

ARTICLE IN PRESS

$[0\ 0]^T$, $\hat{K}_{p0} = [0\ 0\ 0]^T$, $\hat{Q}_m = \text{diag}\,(1\ 1\ 1)$, $R_m = 1$, $\hat{Q}_{ad} = \text{diag}\,(40\ 4\ 8)$ and $\hat{\Gamma} = \text{diag}\,(8\ 8\ 8)$ to make a fair comparison.

Table1 gives the adaptive laws for three cases. For each case, a different adaptive law is introduced since it depends on the input matrix of the plant and the solution of the differential Lyapunov equation. Therefore, the adaptive law changes according to whether a linear or nonlinear model is used as a reference model or plant model.

Fig.6 represents the state trajectories of three different MRAC cases. It can be seen that the NLRM-NLPM adaptation law Case-I enables the plant model response to follow almost perfectly the reference model response except for the first second of the transient region. Additionally, the time response of Case-II is also compared with

Table 1: Parameter details of the adaptive laws (mechanisms)

		$\check{B}_p(x_p)$		$P_{ad}(x_p,x_m)$		States	
Case No.	Adaptation law	V[a]	C[b]	V	C	x_p	x_m
Case-I	Eq. (27)	✓		✓			NLRM
Case-II	Eq. (29)	✓			✓	NLPM	LRM
Case-III	Eq. (31)		✓		✓		LRM

[a]V denotes varying, i.e., a state-dependent matrix. [b]C denotes constant, i.e., a constant matrix.

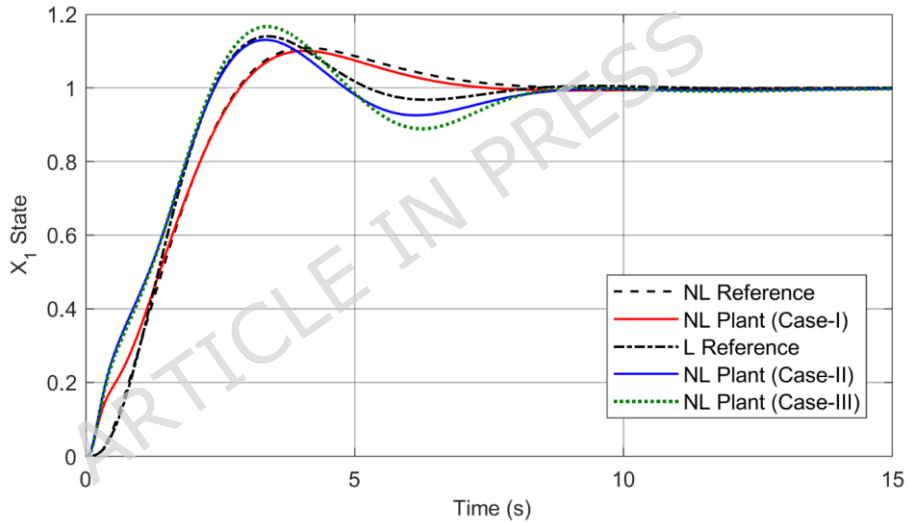


Fig. 6: NLPM response with both LRM and NLRM

that of Case-III. The comparison shows that the Case-II provides lower overshoot and slightly lower settling time than the Case-III. This difference stems from the way that the input matrix is formed. In Case-II, the input matrix of the plant is a state dependent matrix-valued function, i.e. $\check{B}_p(\hat{x}_p)$, whereas it is a constant matrix $\check{B}_p$ in

ARTICLE IN PRESS

Case-III. Therefore, the adaptation law in Case-II tends to adapt itself more readily to the changes in the response of the LRM. Although both cases yield acceptable tracking performance, they are not able to reach the performance level achieved in the Case-I according to the results of the comparison made under the same conditions.

The overall quality of the time responses for the three cases are also determined through the performance indices. These indices are selected from the most commonly used error performances: Integral Square Error-ISE, Integral Absolute Error-IAE and Integral Time Absolute Error-ITAE. The indices are defined with *n*-state of interest as follows:

Table 2: Performance evaluation of MRACs according to controller types

Controller	Time response characteristics			PI*		
Type	ST* (s)	OS* (%)	RT* (s)	ISE	IAE	ITAE
Case-I	5.59	10.10	2.19	0.11	1.10	20.70
Case-II	7.15	13.10	1.88	0.36	2.18	41.16
Case-III	7.51	16.70	1.85	0.42	2.54	48.91

*ST: settling time; OS: overshoot; RT: rise time; PI: performance index.

Given $e(t) = [\, e_1\, e_2\, e_3 \cdots e_n\,]^{\top}$ where $e_i = x_i - x_{di}\,(i = 1,2,3,\cdots,n)$ is i^{th} error state between i^{th} state x_i and i^{th} reference state x_i.

$$ISE = \int_{t_0}^{t_f} \{e^2_1(t) + e^2_2(t) + e^2_3(t) + \cdots + e^2_n(t)\}dt$$

$$IAE = \int_{t_0}^{t_f} \{|e_1(t)| + |e_2(t)| + |e_3(t)| + \cdots + |e_n(t)|\}dt$$

$$ITAE = \int_{t_0}^{t_f} t\{|e_1(t)| + |e_2(t)| + |e_3(t)| + \cdots + |e_n(t)|\}dt$$

A single-error value is obtained by summing all the elements of the error vector in the state-space representation to evaluate the performance indices. The values of the performance indices and the measures of the transient response characteristics from Fig.6 are given in Table2. Case-I provides the most successful performance in all evaluation criteria except rise time. Therefore, the most suitable MRAC architecture for the unknown plants is the one used in Case-I.

ARTICLE IN PRESS

3.1.4 Robustness Analysis of the proposed MRAC (Monte Carlo Simulations)

Following the analyses described above, the question of to what extent a system controlled by the MRAC approach is affected by parametric uncertainties is also addressed. For this purpose, Monte Carlo Simulations are performed using the NLRM (23), the LRM (28) and the uncertain NLPM

$$\dot{x}_{p1} = x_{p2}$$
$$\dot{x}_{p2} = -\alpha_1 x_{p1} e_{xp1} + \alpha_2 x_{2p2} + \alpha_3 e_{xp1} u_p \quad (33)$$

where α_1,α_2 and α_3 are the uniformly distributed random numbers in the interval (1, 10). For each reference model, 50 different simulations are performed with the uncertain NLPM (33) for the step, sawtooth, and sinusoidal wave commands separately

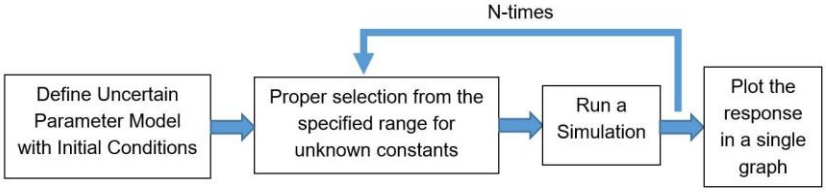


Fig. 7: The basic concept of the Monte-Carlo approach for uncertain parametric models.

Table 3: Statistical data of the Monte-Carlo simulations for uncertain parameters in the interval (1,10)

	N	Min-Val.	Max-Val.	Mean	Variance	Std. Dev.
α_1	50	1.31	9.97	5.21	7.20	2.68
α_2		1.29	9.64	5.53	5.71	2.39
α_3		1.11	9.74	5.17	7.20	2.68

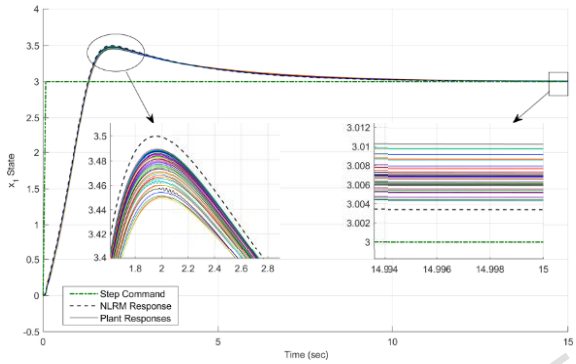
in ~~MatLAB~~ MATLAB R2018a. Monte Carlo Simulations for the uncertain parametric models are shown as a flow chart in Fig. 7. Descriptive statistical data for the uncertain parameters from 50 simulation results are given in Table 3.

The state trajectories $x_{p1}(t)$ obtained from Monte Carlo simulations are respectively shown in Fig.8 and Fig.9 for the MRAC approaches with the NLRM and the LRM. From Fig.8 and Fig.9, it is clearly seen that the closed-loop system controlled by the MRAC approach with the LRM is more sensitive to the parameter uncertainty than that with the NLRM. Therefore, it can be said that the MRAC system with NLRM ~~is more robust than the counterpart with LRM.~~ shows successful tracking

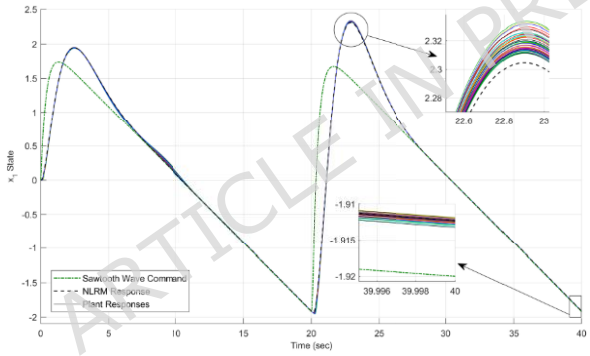
ARTICLE IN PRESS

performance under parametric uncertainties than the counterpart with LRM. In addition, the proposed MRAC approach exhibits better transient response performance, especially for the step and sawtooth commands. On the other hand, a similar interpretation can not be made for the sine wave command because the sine wave command does not include sharp changes over time, and therefore the MRAC approach with LRM is also able to achieve the desired command-following task successfully.

In the further analysis, it has been observed that in some random selections of the coefficients, the uncertain NLPM can not be controlled by the MRAC approach with the linearized reference model when a sawtooth and step command is applied. As an example, some unsuccessful results are given in Fig.10. Of the plants with parametric uncertainties, 16 and 11 out of 50 are not able to be controlled by the MRAC approach with the LRM (28) for the sawtooth wave and step commands, respectively.



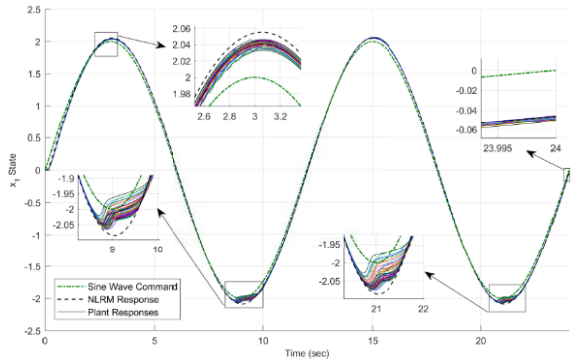
(a) Step Command



(b) Sawtooth Wave Command

ARTICLE IN PRESS

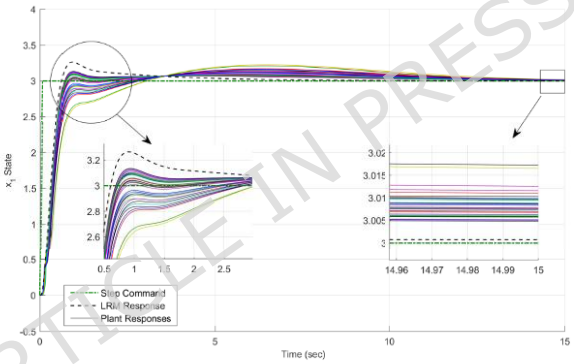
ARTICLE IN PRESS



(c) Sine Wave Command

Fig. 8: Responses of uncertain NLPM controlled by MRAC approach with NLRM

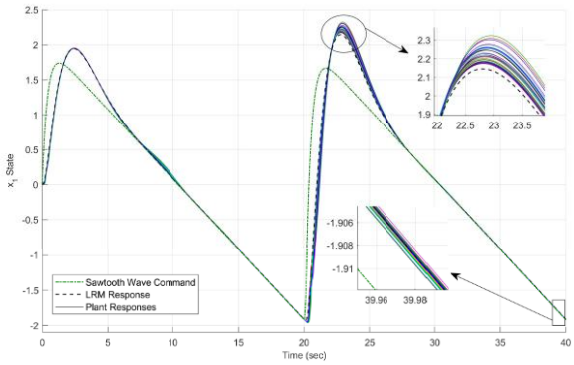
On the contrary, it is shown in Fig- 8 that MRAC approach with the NLRM enable the plant state trajectory to follow the state trajectory of the NLRM with a slight inaccuracy in the transient response phase. These results, which can be considered as indicators, are striking and support the use of the NLRM rather than the LRM for controlling uncertain systems.



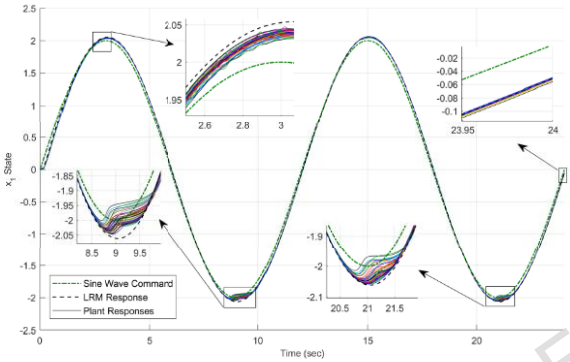
(a) Step Command

ARTICLE IN PRESS

ARTICLE IN PRESS

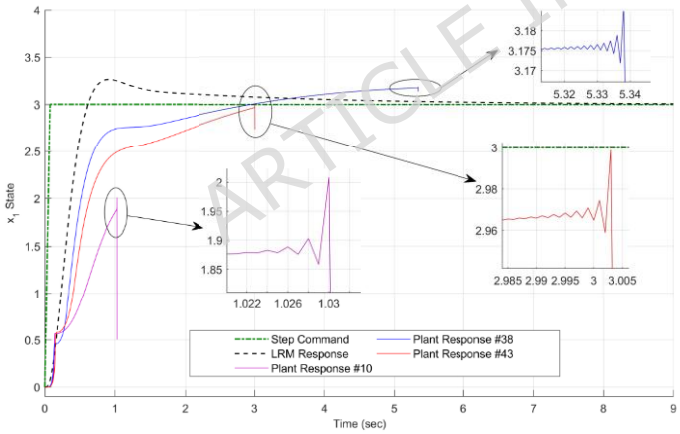


(b) Sawtooth Wave Command



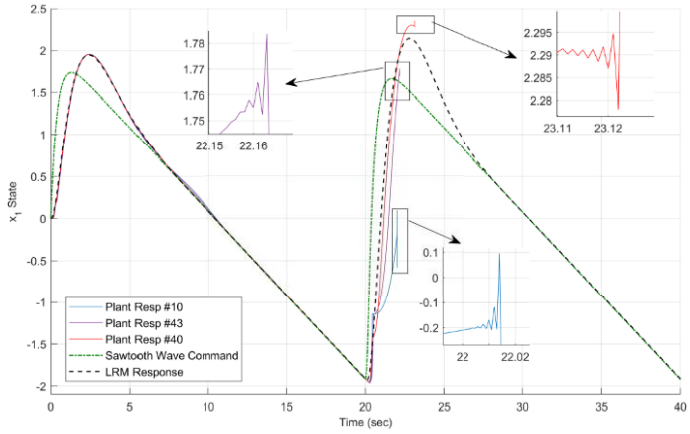
(c) Sine Wave Command

Fig. 9: Responses of uncertain NLPM controlled by MRAC approach with LRM



(a) Step Command

ARTICLE IN PRESS



(b) Sawtooth Wave Command

Fig. 10: Diverged responses of uncertain NLPM controlled by MRAC approach with LRM

Additionally, the q_1,q_2,q_3 parameters forming $Q_{ad}^{\wedge} = diag(q_1,q_2,q_3)$ and the parameter gamma (γ, modelled as an integer) forming $\Gamma = \gamma * diag(1,1,1)$, are randomly varied using a normal (Gaussian) distribution within intervals of ±20% and ±25%, respectively, for a system that was previously stable under the operating conditions at the designated point. Similarly, the coefficients α_1,α_2, and α_3 in (25) are randomly varied in each simulation to follow a Gaussian distribution within the range of (1,10). The analyses reveal that the adaptive controller is highly dependent on both the input signal type (step and sawtooth) and the reference system configuration (Case-I/NLRM and Case-II/LRM). According to the findings of the uncertainty analysis across N = 250 cumulative simulations reported in Table 4, the system achieved a success rate of 99.6% under a step input with the Case-I configuration. However, when switched to the Case-II configuration, the system's success rate dropped to 74.8%, demonstrating inadequate control performance across 63 simulations (Run Crash Count).

Applying a sawtooth input signal with sharper transitions increased the system's dynamic load, leading to noticeable degradation in the adaptive controller's statetracking performance. In the Case-I scenario, the system's success rate decreased to 81.2%, resulting in 47 crashes. In contrast, in the Case-II scenario, the system reached its operational limit, failing in nearly half of the trials, with 49.2% of the simulations (123 crashes) failing. This outcome indicates that the combination of the Case-II configuration and the sawtooth input characteristic results in the worst control performance for the system.

ARTICLE IN PRESS

From a statistical distribution perspective, the convergence of the overall mean percentage errors (MPE) and the median values of the $\hat{Q}_{ad}$ parameters toward zero across all scenarios confirms that the random selection mechanism used in the simulation has a symmetric, unbiased distribution. Furthermore, the parameters' ability to naturally and fully reach their extreme deviation limits (±20% and ±25%) in all scenarios demonstrates that the conducted robustness analysis successfully tested the boundary conditions. The detailed tables for each simulation run in the analysis are presented in Appendix D.

Although the uncertainties introduced in the simulation studies are parametric and not direct representations of real-world uncertainties, the results demonstrate that the proposed controller exhibits superior ~~robustness~~ tracking performance under the parametric uncertainties compared to conventional approaches. This suggests that the controller has the potential to handle real-world variations and disturbances effectively. To further support this claim, a set of experiments has been conducted on a twinrotor laboratory helicopter, which inherently suffers from an imbalance between the thrusts produced by its rotors. The experimental results, presented in the following section, provide additional validation of the controller's real-world applicability. ~~and robustness.~~

3.2 Experimental Evaluation

3.2.1 Helicopter Model and Controller Design

In this study, a test-bed manufactured by Quanser Inc. is used as an experimental setup to test the developed control technique. This three-DoF helicopter system has been widely used to validate the advanced controller experimentally due to the control related challenges arisen from its underactuated and cross-coupling dynamics together with the uncertainties in modelling of aerodynamic characteristics and unknown external disturbances [43–45].

The movement of the helicopter is controlled by front and back propellers driven by DC motors. These propellers are mounted parallel to each other so that the test-bed can be identical to a tandem helicopter configuration. The laboratory helicopter has three degrees of freedom to move in the elevation, pitch, and travel axes. The positive directions of these axes are illustrated in Fig.11. A counterweight is placed at the

Table 4: Statistical data of Monte-Carlo simulations for bounded random selections of $\hat{Q}_{ad}$ and $\hat{\Gamma}$.

		Step Input		Sawtooth Input	
		Overall (N=250)		Overall (N=250)	
P_*	Descriptions	w NLRM	w LRM	w NLRM	w LRM
q1	Mean Percentage Error	1.10	-0.60	0.80	-0.10
	Min Deviation (%)	-19.00	-19.30	-18.90	-19.00
	Max Deviation (%)	18.80	19.30	18.90	19.20

ARTICLE IN PRESS

	Median (%)	1.63	-0.53	1.12	-0.65
q2	Mean Percentage Error	0.60	-0.40	0.50	-0.20
	Min Deviation (%)	-19.00	19.20	-19.20	-19.00
	Max Deviation (%)	19.50	19.20	19.50	19.30
	Median (%)	0.46	0.00	0.91	-1.63
q3	Mean Percentage Error	0.90	-0.80	0.50	-0.3
	Min Deviation (%)	-19.30	-19.10	-19.20	-18.90
	Max Deviation (%)	19.60	19.30	19.60	19.40
	Median (%)	0.40	-0.08	-0.25	-0.08
γ	Mean Percentage Error	0.20	0.10	-0.30	0.60
	Min Deviation (%)	-25.00	-25.00	-25.00	-25.00
	Max Deviation (%)	25.00	25.00	25.00	25.00
	Median (%)	-3.75	-1.25	-3.33	0.00
	Run Crash Count	1	63	47	123
	System Success Rate	99.6%	74.8%	81.2%	50.8%

*P: Parameters.

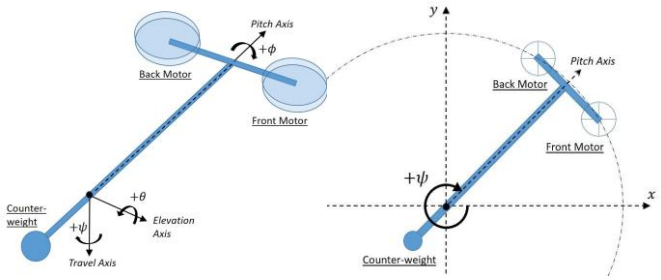
opposite side of the arm with multiple specific (adjustable) locations to balance the weight of the helicopter body with various trim conditions and lift forces (to change the effective mass of the helicopter system). The whole structure is shown in Fig.12. The elevation motion is controlled by the lift force provided by the front and back motors producing the same amount of thrust in the same direction. The pitching movement is obtained by producing a different amount of thrust in the same or opposite direction. Depending on the position of the helicopter's pitching motion, the travel motion is performed.

In the proposed MRAC architecture, the nonlinear model of the plant, i.e., the 3 DoF prototype helicopter, is employed as the nonlinear reference model that generates the desired trajectory to be followed by the plant. A mathematical model has already been derived for a Quanser 3 DoF helicopter by using an identification tool based on frequency response methods, known as CIFER developed by U.S. Army/NASA

Rotorcraft division at Ames Research Center [47, 48]. In this modelling approach, it is considered that the response characteristics of the actuators mounted on the prototype helicopter can be reliably represented by the dynamic behaviour of a firstorder system when input voltages are applied to DC motors. The first-order model sufficiently exhibits the dynamics of the rotor thrust in the presence of the inertial and electric motor

ARTICLE IN PRESS

lag. The combination of these voltage inputs produce movements in the travel and elevation axes. This approach enables the thrust coefficient required in DC



(a) Isometric View (b) Top View

Fig. 11: Positive definitions of the axes (Elevation-θ, Pitch-ϕ and Travel-ψ axes)

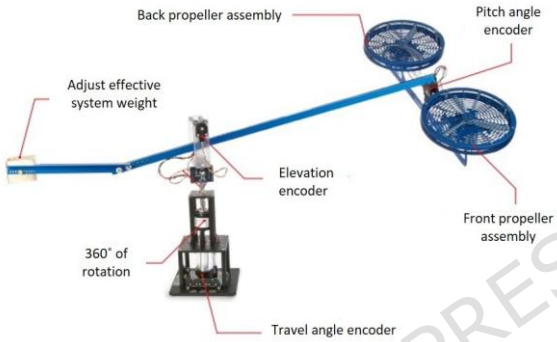


Fig. 12: A 3-DoF helicopter by Quanser Inc.[46]

motor modelling to be disregarded, thereby reducing the complexity of the nonlinear model.

The rolling moment in the pitch axis is called "cyclic torque", and the lifting moment in the elevation axis is called "collective torque". The positive cyclic and collective torques are produced with positive voltages (i.e., $V_b - V_f \triangleq V_{cyc}$ and $V_b + V_f \triangleq V_{coll}$).

The coupled nonlinear dynamic equations are expressed as follows [49]:

$$\ddot{\psi} = -a_1\dot{\psi} + a_2(\beta\tau_{coll} + 1)\sin\phi$$

$$\ddot{\phi} = -b_1\dot{\phi} - b_2\sin\phi - b_3\tau_{cyc}$$

$$\ddot{\theta} = -d_1\dot{\theta} - d_2\sin\theta + d_3\tau_{coll}\cos\phi \quad (34)$$

$$\dot{\tau}_{cyc} = -c_1\tau_{cyc} + 0.5c_2(V_b - V_f)$$

$$\dot{\tau}_{coll} = -e_1\tau_{coll} + 0.5e_2(V_b + V_f)$$

where the constant coefficients of the model parameters are given in Table5.

ARTICLE IN PRESS

The linear reference model is obtained by linearizing the nonlinear model given with (34) at the hover position. The linearization process is performed with Taylor [10] series expansion. Then, the linearized reference model equations become [49]:

Table 5: Nonlinear mathematical model parameters of the 3DoF helicopter [49].

Parameter	a_1	a_2	b_1	b_2	b_3	c_1	c_2
Value	0.2517	0.2105	0.3290	1.5664	16.2	7.32	1
Parameter	d_1	d_2	d_3	e_1	e_2	β	
Value	0.1011	0.504	1.34	6.16	1	4	

$$\begin{aligned}
\ddot{\psi} &= -0.2517\dot{\psi} + 0.1671\phi \\
\ddot{\phi} &= -0.3260\dot{\phi} - 1.4220\phi - 16.2\tau_{cyc} \\
\ddot{\theta} &= -0.1008\dot{\theta} - 0.5544\theta + 1.34\tau_{coll} \\
\dot{\tau}_{cyc} &= -7.32\tau_{cyc} + 0.95(V_b - V_f) \\
\dot{\tau}_{coll} &= -6.16\tau_{coll} + 1.4(V_b + V_f)
\end{aligned} \tag{35}$$

Given the state and control-input vectors as follows

$$\begin{aligned}
x_m &= \begin{bmatrix} \theta & \phi & \psi & \dot{\theta} & \dot{\phi} & \dot{\psi} & \tau_{cyc} & \tau_{coll} \end{bmatrix}^\top \\
&= \begin{bmatrix} x_{m_1} & x_{m_2} & x_{m_3} & x_{m_4} & x_{m_5} & x_{m_6} & x_{m_7} & x_{m_8} \end{bmatrix}^\top \\
u_m &= \begin{bmatrix} V_f & V_b \end{bmatrix}^\top = \begin{bmatrix} u_{m_1} & u_{m_2} \end{bmatrix}^\top
\end{aligned}$$

the nonlinear model (34) can be rewritten in the following form:

$$\begin{aligned}
\dot{x}_{m1} &= x_{m4} \quad \dot{x}_{m2} = x_{m5} \quad \dot{x}_{m3} = x_{m6} \\
\dot{x}_{m4} &= -d_1 x_{m4} - d_2 \sin(x_{m1}) + d_3 x_{m8} \cos(x_{m2}) \quad \dot{x}_{m5} = -b_1 x_{m5} - b_2 \sin(x_{m2}) - b_3 x_{m7} \\
\dot{x}_{m6} &= -a_1 x_{m6} + a_2(\beta x_{m8} + 1)\sin(x_{m2}) \quad \dot{x}_{m7} = -c_1 x_{m7} + 0.5 c_2(-u_{m1} + u_{m2}) \\
\dot{x}_{m8} &= -e_1 x_{m8} + 0.5 e_2(u_{m1} + u_{m2})
\end{aligned} \tag{36}$$

Considering that the state-space description in (36) can be rewritten in the form of

$$\dot{x}_m = f(x_m) + B_m(x_m)u_m \tag{37}$$

ARTICLE IN PRESS

ARTICLE IN PRESS

the extended linearisation approach is applied to factorize the state-space description (37) into a linear-like structure as follows:

$$\dot{x}_m = A_m(x_m)x_m + B_m(x_m)u_m \tag{38}$$

Since the parametrization is not unique for multivariable case [40], the equivalent representation of the 3 DoF helicopter model (38) is given by the state-dependent system matrix

$$A_m(x_m) = \begin{bmatrix} 0_3 & I_3 & 0_{3\times 2} \\ A_{21} & A_{22} & A_{23} \\ 0_{2\times 3} & 0_{2\times 3} & A_{33} \end{bmatrix} \tag{39}$$

$$A_{21} = \begin{bmatrix} 0 & D(x_m) & 0 \\ 0 & 0 & E(x_m) \\ 0 & F(x_m) & 0 \end{bmatrix}, A_{22} = -\begin{bmatrix} 0 & d_1 & 0 \\ 0 & 0 & b_1 \\ 0 & 0 & a_1 \end{bmatrix}$$

$$A_{23} = \begin{bmatrix} 0 & G(x_m) \\ -b_3 & 0 \\ 0 & e_1 \end{bmatrix}, A_{33} = -\begin{bmatrix} 0 & 0 \\ 0 & 0 \end{bmatrix}$$

where $D(x_m) = -d_2 \sin(x_{m1})(x_{m1})^{-1}$, $G(x_m) = d_3 \cos(x_{m2})$, $F(x_m) = a_2(\beta x_{m8} + 1)\sin(x_{m2})(x_{m2})^{-1}$ and $E(x_m) = -b_2 \sin(x_{m2})(x_{m2})^{-1}$. It is worth noting here that $\sin(x_m)/x_m$ converges 1 as x_m tends to zero, and therefore the terms $D(x_m)$, $E(x_m)$ and $F(x_m)$ become

$$D(x_m) = -d_2, E(x_m) = -b_2 \text{ and } F(x_m) = a_2(\beta x_{m8} + 1)$$

The constant control-input matrix is given below

$$B_m = \begin{bmatrix} 0 & \cdots & 0 & -0.5c_2 & 0.5c_2 \\ 0 & \cdots & 0 & 0.5e_2 & 0.5e_2 \end{bmatrix}^\top$$

Since the elevation and travel angles are desired to be controlled, the output states, y_m is determined as follows.

$$y_m = C_m x_m = \begin{bmatrix} 1 & 0 & 0 & 0 & \cdots & 0 \\ 0 & 0 & 1 & 0 & \cdots & 0 \end{bmatrix} x_m$$

The NLRM can be augmented by introducing the integral states in order to perform a tracking task with SDRE approach [50, 51] according to A. Thus, the controller design is completed to achieve the tracking task. It is worth noting that the controllability of the augmented system is guaranteed when $x_{m1}, x_{m2} \in (-\pi/2, \pi/2)$ are satisfied.

ARTICLE IN PRESS

ARTICLE IN PRESS

3.2.2 Initial Positions and Selected Values

The initial values for the 3 DoF helicopter setup is determined as $\theta_0 = -15^\circ$, $\psi_0 = 0^\circ$, and $\phi_0 = 0^\circ$ for the elevation, pitch and travel axes, respectively. Their derivatives are taken all zero at the initial position.

The NL and linearised models of the helicopter test-bed derived are used as the reference model for the proposed MRAC design. For the command-following task, SDRE control method is applied to stabilise the NL reference model whereas LQR method is applied for controlling the linearised reference model. Hence, it is guaranteed that the reference model outputs are bounded in the proposed MRAC architecture.

The effective control of the experimental setup depends on the proper selection of parameter values of the weighting matrices. The selection of a weighting matrix in the design of LQR controller can be made by using an optimization method. Yet, any exact method has not been found for the selection of the weighting matrix in the SDRE method. In the real-time application of this study, the weighting matrices are selected to have a reasonable response to meet the required control performance criteria. The same method was also used to find the learning rate, Γ. Additionally, the selection of the weighting matrix, Q_m, used for the feedback law stabilizing the reference models was made in consideration of reducing the overshoot values.

The weighting matrices required to compute the optimal control laws and the adaptive laws are selected to be diagonal matrices. The weighting matrices and the learning rate, Γ selected for the experimental study are given as follows

$$\hat{Q}_m = \mathrm{diag}(150,5,250,5.10^4,10,15,1,1,100,5)\ \hat{Q}_{ad} = \mathrm{diag}(200,1,50,40,1,20,1,1,1,2)$$

$$R = \mathrm{diag}(1,1)$$

$$\Gamma = 12\hat{} * \mathrm{diag}(1,1,1,1,1,1,1,1,1,1)$$

In this study, all weighting matrices are used the same for both linear and nonlinear models to make a fair comparison. The sampling frequency (f_w) is chosen as 100 Hz.

3.2.3 Discussion on Experimental Results

The time responses of the helicopter test-bed to step commands in the elevation and travel axes are examined. The desired trajectory for the helicopter is described as follows. At first, the helicopter is lifted by 15° on the elevation axis to hold it at the hover position as shown in the Fig.13. Then, a 15-degree turn is made to be in the negative direction of the travel axis on the constant elevation. After that, the desired elevation angle is set to 10°. Finally, a 20-degree turn is made in the positive direction of the travel axis on the constant elevation again. In order for the plant response to follow the reference model response more easily, the step commands are ramped up with a constant rate of 80°, approximately. The experimental results for the elevation (θ) and travel (ψ) axes are given in Fig.13 and Fig.14, respectively.

ARTICLE IN PRESS

As seen in Fig.13, the behaviour of the 3 DoF helicopter in elevation axis is more aggressive (agile) due to the selected weighting matrix, so that the plant is able to follow the reference trajectory almost exactly in the first 10 seconds. However, the agility affects the rise time. For this reason, the error value of the elevation state increases in the transient region when the step command is applied at the 80th second. Since the proposed MRAC architecture with the NLRM enables the error between the responses of the plant and reference systems to be decreased to the acceptable level, the elevation angle settles to the desired trajectory in the elevation axis. The reason why small fluctuations are seen for a certain period is that step commands in travel axis are applied at the 40th and 120th seconds. However, these undesired effects disappear within 15-20 seconds. Also, the maximum overshoot for the given two-step commands are about 14%. In addition, the settling time is in the range of 25-30 seconds.

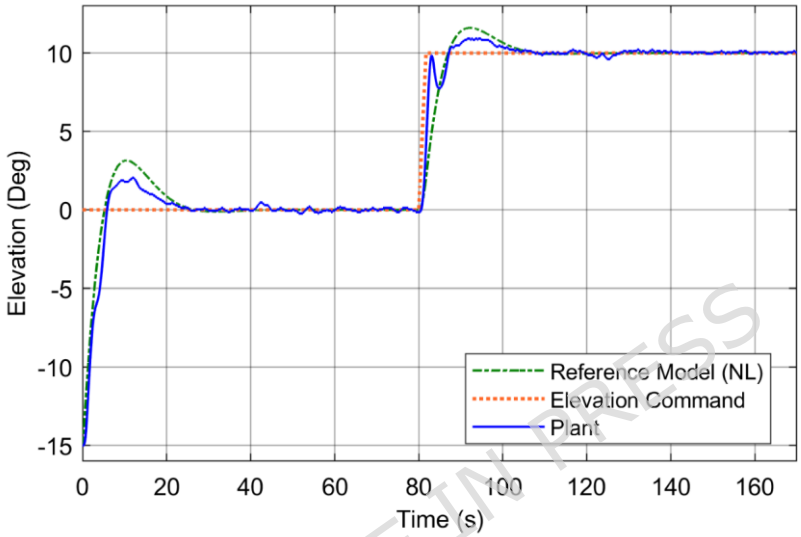


Fig. 13: Time response of the plant with its NLRM (38) on the elevation axis

The travel response of the test-bed is given in Fig.14. A damped oscillation in the first 15 seconds is observed by the effect of the initial command given in the elevation axis. A similar fluctuation appears in the interval of 80-95 seconds when the elevation position is changed. These unintentional effects are suppressed within 15-20 seconds by the adaptive controller. The reference model response to the command at the 40th second is noticeably followed by the plant response, including the transient region. Similarly, a successful tracking performance is achieved for a desired 20-degree turn at the 120th second. The maximum overshoot values for the given two-step commands are also about 16% and the settling time is in the range of 35-40 seconds. These experimental results reveal that the application of the MRAC to the test-bed is done successfully and the proposed MRAC method enables the prototype helicopter to track

ARTICLE IN PRESS

the reference response in the travel axis with better performance than that in the elevation axis.

The controller inputs with the linear and NL references are given in Fig.15. It is seen that the NL reference instead of the linear counterpart provides less motor voltage in this particular example, especially in front motor input. This result shows that using the SDRE-based controller strategy with a NLRM provides an additional adaptation (because of updated $P(x)$ in (22)) together with a suitable learning rate. Note that such an additional adaptation is not introduced for linear reference model because of constant P in the adaptation rule (29), which results in more motor voltage.

Fig.16 and Fig.17 compare the attitude responses of 3 DoF helicopter to step commands in the elevation and travel axes applied to L and NL reference models introduced in MRAC architecture. In Fig.16, the fluctuations of the NLPM response appear smaller when the NLRM is employed rather than the LRM. Additionally, the NLRM produces relatively lower maximum overshoot.

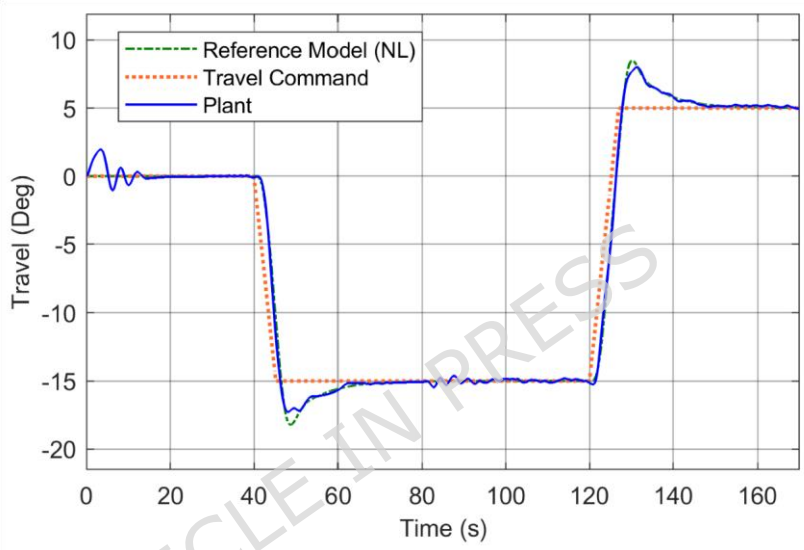


Fig. 14: Time response of the plant with its NLRM (38) on the travel axis

Table 6: Performance evaluation of adaptive controllers according to the selected reference model

Reference Model Type	Time response characteristics						PI* (×10³)		
	ST (s)		OS (%)		RT (s)		ISE	IAE	ITAE
	Elev	Trav	Elev	Trav	Elev	Trav			
L	19.85	21.60	9.30	15.10	1.62	4.90	2.97	11.19	952.52
NL	17.95	19.30	9.30	14.98	1.55	4.70	2.59	9.12	772.87

*ST: settling time; OS: overshoot; RT: rise time; PI: performance index.

ARTICLE IN PRESS

In Table6, the time response characteristics and the performance indices are given separately for the linearized and NL reference models. It is readily apparent that the proposed method with the NLRM provides considerably better results than the traditional one employing a LRM.

In addition, the control input matrix in (38) is generated based on the assumption that the same thrust force can be generated from each rotor when the same voltage input is applied to the DC motors. However, this assumption is not entirely reliable for the 3-DoF helicopter setup utilized in this study. The experimental results in Fig. 18 demonstrate that the helicopter rotates around the travel axis rather than staying in a hover position when the same voltage inputs are simultaneously applied to the DC motors installed in both rotors. This scenario exemplifies the challenging control problems associated with faulty actuator dynamics, thereby validating Assumption 3 for practical applications. Therefore, the experimental results given in Section3.2.3

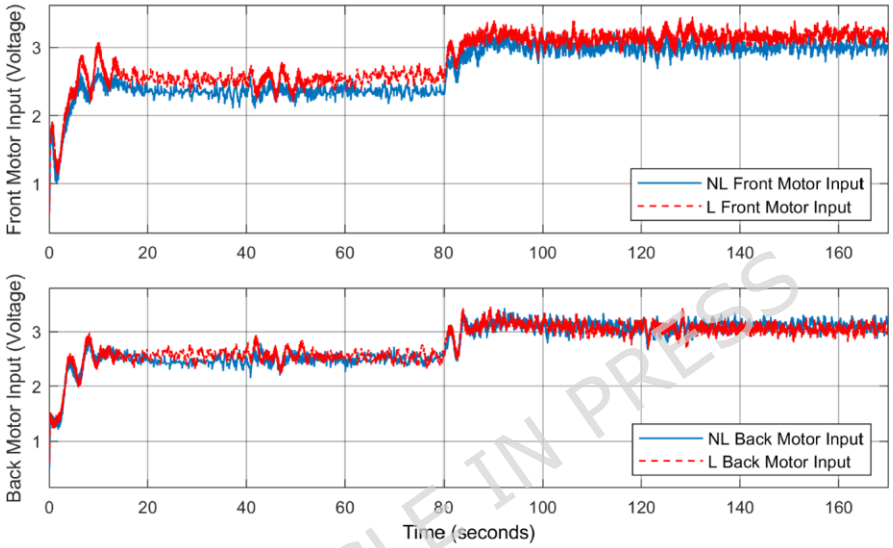


Fig. 15: Comparison of the controller inputs with LRM (35) and NLRM (38).

ARTICLE IN PRESS

also confirm that the proposed approach ~~is robust enough to~~ can deal with the impact of the faulty actuator dynamics.

4 Conclusions

This paper proposes a nonlinear MRAC scheme using a nonlinear reference model rather than a linear reference model, which is usually preferred in a classical MRAC approach, to control uncertain nonlinear plant system. The proposed MRAC approach helps accommodate the uncertainties of the nonlinear plant in a wider range than the

ARTICLE IN PRESS

MRAC approach with the linear reference model. To show the effectiveness of MRAC architecture including nonlinear reference model for nonlinear plants, it is compared against that with linear reference models. The control scheme for the adaptive tracking is first designed based on the error dynamics. Then, three different cases are applied to a second order fictitious nonlinear plant in a simulation environment to examine their control performance. The simulation results show that the proposed MRAC architecture with the nonlinear reference model produces a better tracking performance than the linearised reference model. In addition, ~~the robustness property of the proposed MRAC approach is verified~~ the ability of the proposed MRAC approach to reduce the effects of the parametric uncertainties in the plant is tested through Monte Carlo simulations by comparing it with the MRAC approach with linear reference model. In robustness analysis, it is demonstrated that the MRAC approach with the linear reference model leads to the divergence of the state trajectories of the uncertain plant.

After the simulation studies, the proposed MRAC employing a nonlinear reference model is implemented in real-time to control the 3-DoF prototype helicopter. For the

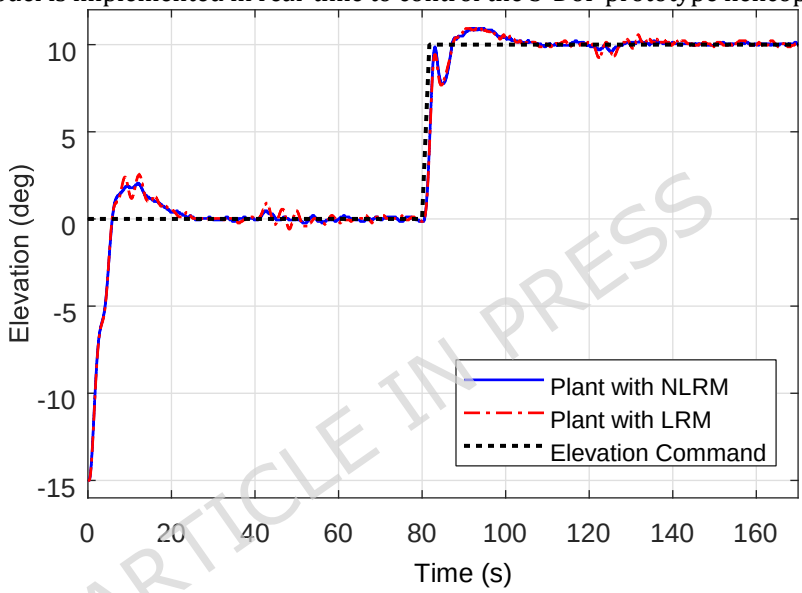


Fig. 16: Comparison of the plant responses with LRM (35) and NLRM (38) for the elevation axis.

ARTICLE IN PRESS

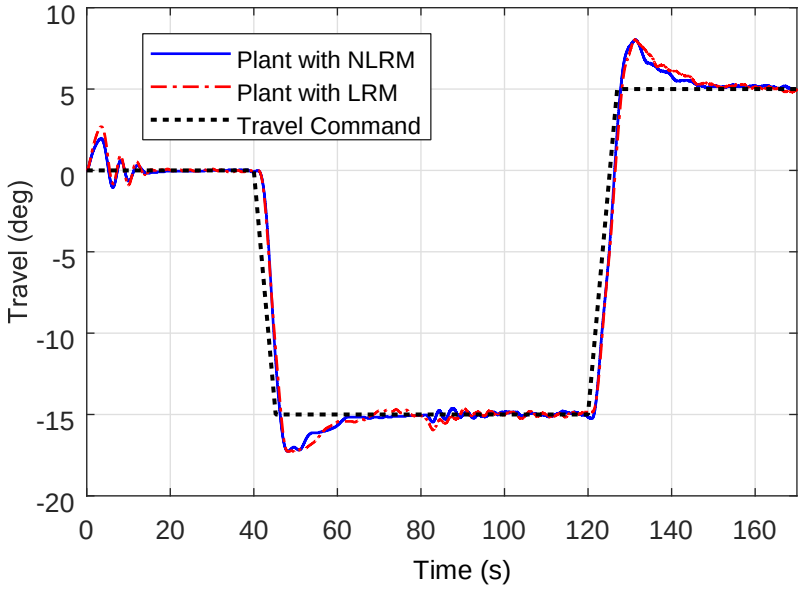


Fig. 17: Comparison of the plant responses with LRM (35) and NLRM (38) for the travel axis.

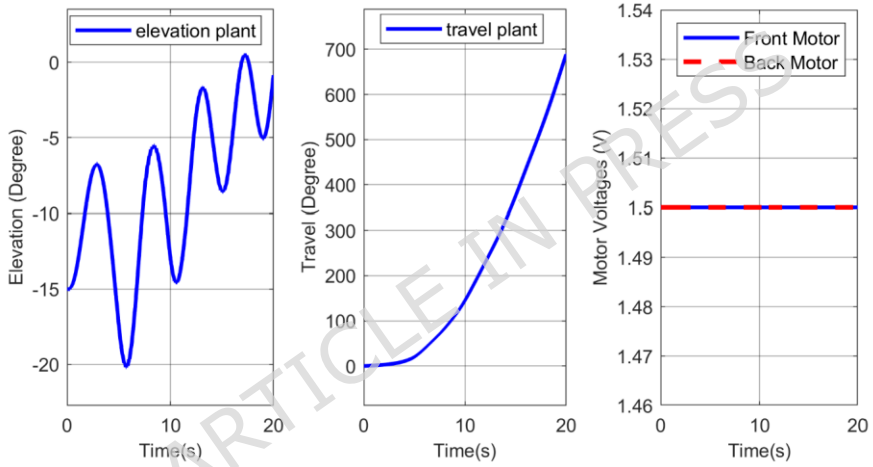


Fig. 18: Plant responses for elevation and travel axes when the same voltage inputs are simultaneously applied to the DC motors.

experimental studies, the nonlinear reference model is derived from the approximation model of the plant, and the SDRE method is applied to the nonlinear reference model to ensure a stable reference model. Experimental results are in line with the simulation results. The results reveal that the proposed method can achieve the tracking objective

ARTICLE IN PRESS

successfully and make the proposed MRAC architecture implementable in real-time for a class of nonlinear MIMO systems. Consequently, the experimental and simulation results reveal that our approach ~~is more robust than the counterparts with a linear reference model against to parametric uncertainties and can also~~ under parametric uncertainties than the counterparts with linear reference models can provide better control performances.

Statements and Declarations

Acknowledgements. There are no acknowledgements.

Conflict of Interest. The authors declare no potential financial or non-financial conflict of interests.

Author Contributions. BMK: Conceptualization, Methodology, Software, Validation, Formal analysis, Investigation, Writing - Original Draft, Visualization **EHC**: Methodology, Software, Validation, Writing - Review & Editing, Visualization **MUS**: Conceptualization, Methodology, Writing - Review & Editing, Supervision.

Data Availability. The datasets used and/or analysed during the current study available from the corresponding author on reasonable request.

Funding. No funding.

Supporting Information. The authors declare no supporting information.

Appendices

All controllers throughout the study were carried out using the integralservomechanism design method. The well-known method [52] is presented in Appendix A to ease the reader's access. Controllability matrices related to the simulation studies are given in Appendix B and Appendix C.

Appendix A Command-Following Controller Design for State Dependent Systems

The goal is here to design a controller for desired system outputs to track external reference inputs, so a type-1 servomechanism controller design is considered here. A system is given in following SDC form

$$\dot{x}(t) = A(x)x + B(x)u,\ x(t) = [x_c | x_{nc}]^\top$$

where $x_c(t) \in \mathrm{R}^h$ are the states to be controlled and $x_{nc}(t) \in \mathrm{R}^{(n-h)}$ are the remaining states. Firstly, the output states (control-states) can be defined as $x_c = Cx$, where $C \in \mathrm{R}^{h\times n}$. Then, the given system can be augmented by new integral state vector, $\eta(t) \in \mathrm{R}^h$ to perform a tracking task [50, 51]. In so doing, an augmented system state vector based on an error of the control-states are created as

ARTICLE IN PRESS

$$\hat{x} = [\,(x_c - r) \mid x_{nc} \mid \eta\,]^\top \in \mathbb{R}^{(n+h)},\ \eta(t) = \int (r_d - x_c)dt$$

where external input (command) vector, $r_d \in \mathbb{R}^h$. This augmentation yields the following SDC form of the system

$$\dot{\hat{x}} = \hat{A}(\hat{x})\hat{x} + \hat{B}(\hat{x})\bar{u}$$

where

$$\hat{A}(\hat{x}) = \begin{array}{c|c} A(\hat{x}) & 0_{n\times h} \\ \hline -C & 0_{h\times h} \end{array}, \quad \hat{B}(\hat{x}) = \begin{array}{c} B(\hat{x}) \\ \hline 0_{h\times h} \end{array}.$$

The state-feedback control law for the augmented system, i.e. $\bar{u} = -\hat{K}\hat{x}$ with $\hat{K} \in \mathbb{R}^{h\times(n+h)}$, is constructed by any design procedure appropriate for state dependent systems.

Appendix B Controllability of the NLRM (24)

$$x_m(t) = \begin{bmatrix} x_{m_1} & x_{m_2} \end{bmatrix}^\top, B_m(x_m) = \begin{bmatrix} 0 & e^{x_{m_1}} \end{bmatrix}^\top$$

$$A_m(x_m) = \begin{bmatrix} 0 & 1 \\ -e^{x_{m_1}} & 0.5x_{m_2} \end{bmatrix}.$$

Controllability Matrix of the NLRM:

$$M = [B_m(x_m) \mid A_m(x_m)B_m(x_m)] = \begin{array}{c|c} & 0e_{x_{m1}} \\ \hline e_{x_{m1}} & 0.5x_{m2}e_{x_{m1}} \end{array}.$$

where $det(M) = -\exp(2x_{m1})$. Since $\det(M) \neq 0$ in the time interval $t \in [0, t_f]$, M is always a full rank matrix. Thus, the NLRM (24) is fully state controllable.

Appendix C Controllability of the augmented model of the NLRM (24)

$$\hat{x}_m(t) = [x_{m1}\, x_{m2}\, \eta]^\top$$

ARTICLE IN PRESS

$$= [(x_{m1} - r)\ x_{m2} \qquad (r - x_{m1})dt]^{\top},$$

$$\begin{bmatrix} 0 & 1 & 0 \end{bmatrix} \qquad \begin{bmatrix} 0 \end{bmatrix}$$

$$\hat{A}_m(\hat{x}_m) = \begin{bmatrix} -e_{\hat{x}_{m1}} & 0.5\hat{x}_{m2} & 0 \\ -1 & 0 & 0 \end{bmatrix}, \hat{B}_m(\hat{x}_m) = \begin{bmatrix} e_{\hat{x}_{m1}} \\ 0 \end{bmatrix}.$$

Controllability Matrix of the augmented model of the NLRM:

$$\hat{M} = \mathrm{h}\hat{B}_m(\hat{x}_m) \ \ \hat{A}_m(\hat{x}_m)\hat{B}_m(\hat{x}_m) \ \ \hat{A}_{2m}(\hat{x}_m)\hat{B}_m(\hat{x}_m)\mathrm{i}$$

$$\begin{bmatrix} & | & | & \\ & | & | & 0e_{\hat{x}_{m1}}0.5\hat{x}_{m2}e_{\hat{x}_{m1}} \\ & | & | & \end{bmatrix}$$

$$= \begin{bmatrix} \\ e_{\hat{x}_{m1}}0.5\hat{x}_{m2}e_{\hat{x}_{m1}} - e_{\hat{x}_{m1}}(e_{\hat{x}_{m1}} - 0.25\hat{x}_{2m2}) \\ 00 - e_{\hat{x}_{m1}} \end{bmatrix}$$

where $det(\hat{M}) = \exp(3\hat{x}_{m1})$. Since $\det(\hat{M}) \neq 0$ in the time interval $t \in [0, t_f]$, $\hat{M}$ is always a full rank matrix. Thus, the augmented NLRM (24) is fully state controllable.

Appendix D Monte-Carlo simulation results for $Q\hat{}_{ad}$ and $\hat{\Gamma}$

Table D1: Step Input for Case-I (w NLRM)

	Step Input (w NLRM)				N=50		N=250
P_*	Descriptions	Run 1	Run 2	Run 3	Run 4	Run 5	Overall
q1	Mean Percentage Error	-1.20	2.10	1.80	0.60	2.40	1.10
	Min Deviation (%)	-19.20	-19.00	-18.40	-19.10	-19.00	-19.00
	Max Deviation (%)	19.80	17.60	19.70	18.60	18.20	18.80
	Median (%)	-2.89	1.54	1.58	2.35	5.59	1.63
q2	Mean Percentage Error	1.60	1.80	-2.30	1.90	-0.10	0.60
	Min Deviation (%)	-17.80	-18.60	-19.90	-18.90	-19.70	-19.00
	Max Deviation (%)	19.40	19.60	20.00	19.40	18.80	19.50
	Median (%)	0.00	4.10	-4.66	3.27	-0.43	0.46
q3	Mean Percentage Error	3.70	0.90	0.10	-0.20	0.20	0.90
	Min Deviation (%)	-18.30	-19.90	-19.80	-19.10	-19.50	-19.30

ARTICLE IN PRESS

ARTICLE IN PRESS

	Max Deviation (%)	19.50	19.40	19.50	20.00	19.60	19.60
	Median (%)	3.60	1.18	-2.13	-0.49	-0.16	0.40
γ	Mean Percentage Error	3.50	-3.50	3.30	-2.50	0.30	0.20
	Min Deviation (%)	-25.00	-25.00	-25.00	-25.00	-25.00	-25.00
	Max Deviation (%)	25.00	25.00	25.00	25.00	25.00	25.00
	Median (%)	0.00	-12.50	0.00	-6.25	0.00	-3.75
	Run Crash Count	0	1	0	0	0	1
	System Success Rate	100%	98,0%	100%	100%	100%	99,6%

* P: Parameters.

Table D2: Step Input for Case-II (w LRM)

	Step Input (w LRM)				N=50		N=250
P*	Descriptions	Run 1	Run 2	Run 3	Run 4	Run 5	Overall
q1	Mean Percentage Error	1.10	-0.80	0.40	-2.00	-2.00	-0.60
	Min Deviation (%)	-18.60	-19.30	-19.20	-19.90	-19.40	-19.30
	Max Deviation (%)	19.40	19.70	19.50	18.90	19.10	19.30
	Median (%)	0.55	-0.82	1.51	-2.91	-0.97	-0.53
q2	Mean Percentage Error	0.10	0.80	-3.10	0.30	0.10	-0.40
	Min Deviation (%)	-19.40	-19.00	-18.50	-19.70	-19.20	-19.20
	Max Deviation (%)	19.80	19.60	17.40	19.80	19.20	19.20
	Median (%)	-0.01	4.90	-5.60	-0.47	1.17	0.00
q3	Mean Percentage Error	-2.80	1.20	-0.40	-2.40	0.50	-0.80
	Min Deviation (%)	-18.90	-20.00	-17.50	-20.00	-19.30	-19.10
	Max Deviation (%)	19.30	19.30	20.00	18.30	19.80	19.30
	Median (%)	-4.55	3.74	3.65	-3.85	0.62	-0.08
γ	Mean Percentage Error	2.00	3.00	-4.80	-2.30	2.30	0.10
	Min Deviation (%)	-25.00	-25.00	-25.00	-25.00	-25.00	-25.00
	Max Deviation (%)	25.00	25.00	25.00	25.00	25.00	25.00
	Median (%)	0.00	0.00	-6.25	0.00	0.00	-1.25
	Run Crash Count	11	16	17	8	11	63

ARTICLE IN PRESS

ARTICLE IN PRESS

	System Success Rate	78,0%	68,0%	66,0%	84,0%	78,0%	74,8%

* P: Parameters.

Table D3: Sawtooth Input for Case-I (w NLRM)

Sawtooth Input (w NLRM)		N=50					N=250
P*	Descriptions	Run 1	Run 2	Run 3	Run 4	Run 5	Overall
q1	Mean Percentage Error	-2.00	2.10	1.80	1.40	0.60	0.80
	Min Deviation (%)	-19.40	-19.00	-18.40	-18.70	-19.10	-18.90
	Max Deviation (%)	19.10	17.60	19.70	19.20	18.60	18.90
	Median (%)	-0.97	1.54	1.58	1.10	2.35	1.12
q2	Mean Percentage Error	0.10	1.80	-2.30	0.90	1.90	0.50
	Min Deviation (%)	-19.20	-18.60	-19.90	-19.40	-18.90	-19.20
	Max Deviation (%)	19.20	19.60	20.00	19.00	19.40	19.50
	Median (%)	1.17	4.10	-4.66	0.67	3.27	0.91
q3	Mean Percentage Error	0.50	0.90	0.10	1.10	-0.20	0.50
	Min Deviation (%)	-19.30	-19.90	-19.80	-17.90	-19.10	-19.20
	Max Deviation (%)	19.80	19.40	19.50	19.50	20.00	19.60
	Median (%)	0.62	1.18	-2.13	-0.44	-0.49	-0.25
γ	Mean Percentage Error	2.20	-3.70	2.50	0.00	-2.50	-0.30
	Min Deviation (%)	-25.00	-25.00	-25.00	-25.00	-25.00	-25.00
	Max Deviation (%)	25.00	25.00	25.00	25.00	25.00	25.00
	Median (%)	0.00	-8.33	0.00	0.00	-8.33	-3.33
	Run Crash Count	9	12	11	6	9	47
	System Success Rate	82,0%	76,0%	78,0%	88,0%	82,0%	81,2%

* P: Parameters.

ARTICLE IN PRESS

Table D4: Sawtooth Input for Case-II (w LRM)

Sawtooth Input (w LRM)		N=50					N=250
P*	Descriptions	Run 1	Run 2	Run 3	Run 4	Run 5	Overall

ARTICLE IN PRESS

q1	Mean Percentage Error	1.10	0.40	-1.20	-2.00	1.20	-0.10
	Min Deviation (%)	-18.60	-19.20	-19.20	-19.90	-17.90	-19.00
	Max Deviation (%)	19.40	19.50	19.80	18.90	18.30	19.20
	Median (%)	0.55	1.51	-2.89	-2.91	0.50	-0.65
q2	Mean Percentage Error	0.10	-3.10	1.60	0.30	-0.10	-0.20
	Min Deviation (%)	-19.40	-18.50	-17.80	-19.70	-19.60	-19.00
	Max Deviation (%)	19.80	17.40	19.40	19.80	20.00	19.30
	Median (%)	-0.01	-5.60	0.00	-0.47	-2.09	-1.63
q3	Mean Percentage Error	-2.80	-0.40	3.70	-2.40	0.50	-0.30
	Min Deviation (%)	-18.90	-17.50	-18.30	-20.00	-20.00	-18.90
	Max Deviation (%)	19.30	20.00	19.50	18.30	19.80	19.40
	Median (%)	-4.55	3.65	3.60	-3.85	0.76	-0.08
γ	Mean Percentage Error	1.30	-3.30	3.70	-1.50	2.80	0.60
	Min Deviation (%)	-25.00	-25.00	-25.00	-25.00	-25.00	-25.00
	Max Deviation (%)	25.00	25.00	25.00	25.00	25.00	25.00
	Median (%)	0.00	-8.33	8.33	0.00	0.00	0.00
	Run Crash Count	30	22	22	25	24	123
	System Success Rate	40,0%	56,0%	56,0%	50,0%	52,0%	50,8%

* P: Parameters.

ARTICLE IN PRESS

References

[1] Astolfi, A., Karagiannis, D., Ortega, R.: Nonlinear and Adaptive Control with Applications. Springer, London (2008). https://doi.org/10.1007/ 978-1-84800-066-7

[2] Landau, I.D., Lozano, R., M'Saad, M., Karimi, A.: Adaptive Control: Algorithms, Analysis and Applications. Springer, London (2011)

[3] Narendra, K.S., Annaswamy, A.M.: Stable Adaptive Systems. Dover Publications, Mineola, New York (2012)

[4] Nguyen, N.T.: Model Reference Adaptive Control. Springer, Cham (2018)

[5] Guo, J., Tao, G., Liu, Y.: A multivariable mrac scheme with application to a nonlinear aircraft model. Automatica **47**(4), 804–812 (2011)

ARTICLE IN PRESS

[6] Ventura-Hinostroza, H., Rojas-Moreno, A.: Real–time model reference adaptive control of a 3dof robot arm. In: 2019 IEEE XXVI International Conference on Electronics, Electrical Engineering and Computing (INTERCON). IEEE, Lima,Peru (2019). https://doi.org/10.1109/intercon.2019.8853622

[7] Maki, T., Zhao, M., Shi, F., Okada, K., Inaba, M.: Model reference adaptive control of multirotor for missions with dynamic change of payloads during flight. In: 2020 IEEE International Conference on Robotics and Automation (ICRA), pp. 7433–7439. IEEE, Virtual Conference (2020)

[8] Park, B.-J., Pham, P.-T., Hong, K.-S.: Model reference robust adaptive control of control element drive mechanism in a nuclear power plant. International Journal of Control, Automation and Systems **18**(7), 1651–1661 (2020) https://doi.org/ 10.1007/s12555-019-0987-3

[9] Chen, K.-Y.: A new model reference adaptive control with the disturbance observer-based adaptation law for the nonlinear servomechanisms: Siso and mimo systems. Asian Journal of Control **23**(6), 2597–2616 (2021) https://doi.org/10. 1002/asjc.2398

[10] Tian, G., Duan, G.: Robust model reference tracking for uncertain second-order nonlinear systems with application to robot manipulator. International Journal of Robust and Nonlinear Control (2022) https://doi.org/10.1002/rnc.6450

[11] Yucelen, T., Gruenwald, B., Muse, J.A., De La Torre, G.: Adaptive control with nonlinear reference systems. In: 2015 American Control Conference (ACC), pp. 3986–3991. IEEE, Chicago, IL (2015). https://doi.org/10.1109/acc.2015.7171952

[12] Rong, L., Huang, C., Long, L.: Model reference safety-critical adaptive control for nonlinear and switched systems. International Journal of Adaptive Control and Signal Processing **36**(4), 999–1012 (2022) https://doi.org/10.1002/acs.3390

[13] Wang, D., Wang, S., Yuan, S., Cai, B., Zhang, L.: Guaranteed performance control of switched linear systems: A differential-riccati-equation-based approach. Peerto-Peer Networking and Applications **12**(6), 1810–1819 (2019) https://doi.org/ 10.1007/s12083-019-00748-w

[14] Yuan, S., Lv, M., Baldi, S., Zhang, L.: Lyapunov-equation-based stability analysis for switched linear systems and its application to switched adaptive control. IEEE Transactions on Automatic Control **66**(5), 2250–2256 (2021) https://doi.org/10. 1109/tac.2020.3003647

[15] Liu, T., Buss, M.: Model reference adaptive control of piecewise affine systems with state tracking performance guarantees. International Journal of Robust and Nonlinear Control **32**(7), 4129–4148 (2022) https://doi.org/10.1002/rnc.6015

ARTICLE IN PRESS

[16] Xiao, S., Yan, G., Huang, X., Li, R.: Adaptive fault-tolerant tracking control of piecewise affine systems with performance constraint. International Journal of Robust and Nonlinear Control **36**(1), 172–194 (2025) https://doi.org/10.1002/rnc.70121

[17] Copur, E.H., Arican, A.C., Ozcan, S., Salamci, M.U.: An update algorithm design using moving region of attraction for sdre based control law. Journal of the Franklin Institute **356**(15), 8388–8413 (2019) https://doi.org/10.1016/j.jfranklin.2019.08.007

[18] Babaei, N., Salamci, M.U.: Personalized drug administration for cancer treatment using model reference adaptive control. Journal of Theoretical Biology **371**, 24–44 (2015) https://doi.org/10.1016/j.jtbi.2015.01.038

[19] Babaei, N., Salamci, M.U.: Controller design for personalized drug administration in cancer therapy: Successive approximation approach. Optimal Control Applications and Methods **39**(2), 682–719 (2017) https://doi.org/10.1002/oca. 2372

[20] Kocagil, B.M., Ozcan, S., Arican, A.C., Guzey, U.M., Copur, E.H., Salamci, M.U.: Adaptive control of a 3 DoF helicopter with linear and nonlinear reference models. In: 2018 6th International Conference on Control Engineering and Information Technology (CEIT). IEEE, Istanbul,Tu¨rkiye (2018). https://doi.org/10.1109/ceit.2018.8751799

[21] Kocagil, B.M., Ozcan, S., Arican, A.C., Guzey, U.M., Copur, E.H., Salamci, M.U.: MRAC of a 3-DoF helicopter with nonlinear reference model. In: 2018 26th Mediterranean Conference on Control and Automation (MED), pp. 278–283. IEEE, Zadar, Croatia (2018). https://doi.org/10.1109/med.2018.8442941

[22] Babaei, N., Salamci, M.U.: Mixed therapy in cancer treatment for personalized drug administration using model reference adaptive control. European Journal of Control **50**, 117–137 (2019) https://doi.org/10.1016/j.ejcon.2019.03.001

[23] Asiain, E., Garrido, R.: Anti-chaos control of a servo system using nonlinear model reference adaptive control. Chaos, Solitons & Fractals **143**, 110581 (2021) https://doi.org/10.1016/j.chaos.2020.110581

[24] Kreisselmeier, G., Narendra, K.: Stable model reference adaptive control in the presence of bounded disturbances. IEEE Transactions on Automatic Control **27**(6), 1169–1175 (1982) https://doi.org/10.1109/tac.1982.1103093

[25] Dixit, S., Montanaro, U., Dianati, M., Mouzakitis, A., Fallah, S.: Integral mrac with bounded switching gain for vehicle lateral tracking. IEEE Transactions on Control Systems Technology **29**(5), 1936–1951 (2021) https://doi.org/10.1109/ tcst.2020.3024586

ARTICLE IN PRESS

[26] Cos, C.R.d., Dimarogonas, D.V.: Adaptive cooperative control for human-robot load manipulation. IEEE Robotics and Automation Letters **7**(2), 5623–5630 (2022) https://doi.org/10.1109/lra.2022.3158435

[27] Guduri, B., Batra, R.: Robust model reference adaptive controller for atmospheric plasma spray process. SN Applied Sciences **4**(4), 1–10 (2022)

[28] Xiao, S., Niu, N., Chen, Z.: Robust adaptive fault-tolerant tracking control of uncertain piecewise affine systems. International Journal of Systems Science **56**(16), 3986–3998 (2025) https://doi.org/10.1080/00207721.2025.2480745

[29] Yuan, S., De Schutter, B., Baldi, S.: Robust adaptive tracking control of uncertain slowly switched linear systems. Nonlinear Analysis: Hybrid Systems **27**, 1–12 (2018) https://doi.org/10.1016/j.nahs.2017.08.003

[30] C¸imen, T.: State-dependent riccati equation (sdre) control: A survey. IFAC Proceedings Volumes **41**(2), 3761–3775 (2008) https://doi.org/10.3182/20080706-5-kr-1001.00635

[31] Pontryagin, L.S.: Mathematical Theory of Optimal Processes. Routledge, Oxfordshire (2018)

[32] Mracek, C.P., Cloutier, J.R.: Control designs for the nonlinear benchmark problem via the state-dependent riccati equation method. International Journal of Robust and Nonlinear Control **8**(4), 401–433 (1998) https://doi.org/10.1002/ (sici)1099-1239(19980415/30)8:4/5⟨401::aid-rnc361⟩3.0.co;2-u

[33] C¸imen, T.: Systematic and effective design of nonlinear feedback controllers via the state-dependent riccati equation (sdre) method. Annual Reviews in Control **34**(1), 32–51 (2010) https://doi.org/10.1016/j.arcontrol.2010.03.001

[34] Korayem, M.H., Nekoo, S.R.: Finite-time state-dependent riccati equation for time-varying nonaffine systems: Rigid and flexible joint manipulator control. ISA Transactions **54**, 125–144 (2015) https://doi.org/10.1016/j.isatra.2014.06.006

[35] Nekoo, S.R.: Output- and state-dependent riccati equation: An output feedback controller design. Aerospace Science and Technology **126**, 107649 (2022) https://doi.org/10.1016/j.ast.2022.107649

[36] Korayem, M.H., Lademakhi, N.Y.: A suboptimal control scheme based on integrated real-time nonlinear estimation-identification approach for developed flexible joint manipulators structure. Control Engineering Practice **143**, 105779 (2024) https://doi.org/10.1016/j.conengprac.2023.105779

ARTICLE IN PRESS

[37] Jang, J., Annaswamy, A.M., Lavretsky, E.: Adaptive flight control in the presence of multiple actuator anomalies. In: 2007 American Control Conference, pp. 3300–3305. IEEE, New York City,USA (2007). https://doi.org/10.1109/acc.2007. 4282990

[38] Jang, J., Annaswamy, A.M., Lavretsky, E.: Adaptive control of time-varying systems with gain-scheduling. In: 2008 American Control Conference, pp. 3416–3421. IEEE, Washington, USA (2008). https://doi.org/10.1109/acc.2008.4587021

[39] Gajic, Z., Qureshi, M.T.J.: Lyapunov Matrix Equation in System Stability and Control. Dover Publications Inc, Mineola, New York (2008)

[40] C¸imen, T.: Survey of state-dependent riccati equation in nonlinear optimal feedback control synthesis. Journal of Guidance, Control, and Dynamics **35**(4), 1025–1047 (2012) https://doi.org/10.2514/1.55821

[41] Hammett, K.D.: Control of nonlinear systems via state feedback state-dependent riccati equation techniques. PhD thesis, Air Force Institute of Technology, USA (1997)

[42] Sznaier, M., Cloutier, J., Hull, R., Jacques, D., Mracek, C.: Receding horizon control lyapunov function approach to suboptimal regulation of nonlinear systems. Journal of Guidance, Control, and Dynamics **23**(3), 399–405 (2000) https://doi.org/10.2514/2.4571

[43] Makki, O.T., Moosapour, S.S., Mobayen, S., Nobari, J.H.: Design, mathematical modeling, and control of an underactuated 3-dof experimental helicopter. IEEE Access **12**, 55568–55586 (2024) https://doi.org/10.1109/access.2024.3389703

[44] Verginis, C.K., Bechlioulis, C.P., Soldatos, A.G., Tsipianitis, D.: Robust trajectory tracking control for uncertain 3-dof helicopters with prescribed performance. IEEE/ASME Transactions on Mechatronics **27**(5), 3559–3569 (2022) https://doi.org/10.1109/tmech.2021.3136046

[45] Zhu, X., Li, D.: Robust fault estimation for a 3-dof helicopter considering actuator saturation. Mechanical Systems and Signal Processing **155**, 107624 (2021) https://doi.org/10.1016/j.ymssp.2021.107624

[46] Quanser: 3 DOF Helicopter Data Sheet. Quanser Inc (2019)

[47] Tischler, M.B., Cauffman, M.G.: Frequency-response method for rotorcraft system identification: Flight applications to BO 105 coupled rotor/fuselage dynamics. Journal of the American Helicopter Society **37**(3), 3–17 (1992) https://doi.org/10.4050/jahs.37.3.3

[48] Remple, R.K., Tischler, M.B.: Aircraft and Rotorcraft System Identification:

ARTICLE IN PRESS

Engineering Methods With Flight-test Examples. American Institute of Aeronautics and Astronautics, Reston, Virginia (2006). https://doi.org/10.2514/4. 861352

[49] Ishutkina, M.A.: Design and implimentation of a supervisory safety controller for a 3dof helicopter. Master of science, Massachusetts Institute of Technology. Department of Aeronautics and Astronautics (2004)

[50] Cloutier, J.R., Stansbery, D.T.: Control of a continuously stirred tank reactor using an asymmetric solution of the state-dependent riccati equation. In: Proceedings of the 1999 IEEE International Conference on Control Applications
(Cat. No.99CH36328), pp. 893–898. IEEE, Hawaii,USA (1999). https://doi.org/ 10.1109/cca.1999.800904

[51] Stansbery, D., Cloutier, J.: Nonlinear, hybrid bank-to-turn/skid-to-turn missile autopilot design. In: AIAA Guidance, Navigation, and Control Conference and Exhibit, pp. 01–5929. American Institute of Aeronautics and Astronautics, Montreal,Canada (2001). https://doi.org/10.2514/6.2001-4158

[52] Ogata, K.: Modern Control Engineering, 5th edn. Prentice Hall, Upper Saddle River, New Jersey (2010)

ARTICLE IN PRESS